Congenital macrothrombocytopenia with focal myelofibrosis due to mutations in human G6b-B is rescued in humanized mice

Inga Hofmann,[1,2*] Mitchell J. Geer,[3*] Timo Vögtle,[3] Andrew Crispin,[2] Dean R. Campagna,[2] Alastair Barr,[4] Monica L. Calicchio,[2] Silke Heising,[3] Johanna P. van Geffen,[5] Marijke J. E. Kuijpers,[5] Johan W. M. Heemskerk,[5] Johannes A. Eble,[6] Klaus Schmitz-Abe,[7] Esther A. Obeng,[8] Michael Douglas,[9-11] Kathleen Freson,[12] Corinne Pondarré,[13] Rémi Favier,[14,15] Gavin E. Jarvis,[16] Kyriacos Markianos,[2] Ernest Turro,[17] Willem H. Ouwehand,[18-20] Alexandra Mazharian,[3] Mark D. Fleming,[2*] and Yotis A. Senis[3*]

[1]Division of Hematology, Oncology, Bone Marrow Transplantation, Department of Pediatrics, University of Wisconsin, Madison, WI, USA

[2]Department of Pathology, Boston Children's Hospital, Boston, MA, USA

[3]Institute of Cardiovascular Sciences, College of Medical and Dental Sciences, University of Birmingham, Birmingham, UK

[4]Department of Biomedical Science, University of Westminster, London, UK

[5]Department of Biochemistry, Cardiovascular Research Institute Maastricht, Maastricht University, Maastricht, The Netherlands

[6]Institute of Physiological Chemistry and Pathobiochemistry, University of Münster, Münster, Germany

[7]Division of Genetics and Genomics, Boston Children's Hospital, Boston, MA, USA

[8]Dana-Farber/Boston Children's Cancer and Blood Disorders Center, Harvard Medical School, Boston, MA, USA

[9]Institute of Inflammation and Ageing, College of Medical and Dental Sciences, University of Birmingham, Birmingham, UK

[10]Department of Neurology, Dudley Group NHS Foundation Trust, Russells Hall Hospital, Dudley, UK

[11]School of Life and Health Sciences, Aston University, Birmingham, UK

[12]Department of Cardiovascular Sciences, University of Leuven, Leuven, Belgium

[13]Department of Pediatrics, and INSERM Unité 955, Paris-Est Créteil University, Créteil, France

[14]Assistance Publique-Hôpitaux de Paris, French reference centre for platelet disorders; A Trousseau Children Hospital Paris, France

[15]Gustave Roussy Institute, UMR 1170, Villejuif, France

[16]Department of Physiology, Development and Neuroscience, University of Cambridge, Cambridge, CB2 3EG, UK

[17]Department of Haematology and MRC Biostatistics Unit, University of Cambridge, Cambridge, UK

[18]Wellcome Trust Sanger Institute, Wellcome Trust Genome Campus, Hinxton, United Kingdom.

[19]Department of Haematology, University of Cambridge, Cambridge Biomedical Campus, Cambridge, United Kingdom

[20]NHS Blood and Transplant, Cambridge Biomedical Campus, Cambridge, United Kingdom

*contributed equally

Corresponding authors:
Inga Hofmann, MD, Assistant Professor of Pediatrics, University of Wisconsin, Madison, UW Health, WIMR 4151, 1111 Highland Avenue, Madison, WI 53705
Email: ihofmann@wisc.edu
Phone: (608) 263-6405
Fax: (608) 265-9721

Yotis Senis, PhD, Professor of Cellular Haemostasis, University of Birmingham, Birmingham, UK, B15 2TT
Email: y.senis@bham.ac.uk
Phone: +44 (0)121 414 8308

Word count:
Abstract: 216
Manuscript: 4480
Figures/Tables: 6/2
Supplemental Figures: 15
Supplemental Material:
References: 50

Running title: Congenital Myelofibrosis due to G6b-B Mutations

Key words: myelofibrosis, congenital myelofibrosis, familial myelofibrosis, myeloproliferative neoplasm, C6orf25, MPIG6B, G6b-B, megakaryocytes, platelets, thrombocytopenia, transgenic mouse

Key Points

- Autosomal recessive loss-of-function mutations in G6b-B (*MPIG6B*) cause congenital macrothrombocytopenia with focal myelofibrosis (cMTFM).
- G6b-B has orthologous physiological functions in human and mice regulating megakaryocyte and platelet production and function.

Abstract

Unlike primary myelofibrosis (PMF) in adults, myelofibrosis in children is rare. Congenital (inherited) forms of myelofibrosis (cMF) have been described, but the underlying genetic mechanisms remain elusive. Here we describe 4 families with autosomal recessive inherited macrothrombocytopenia with focal myelofibrosis due to germline loss-of-function mutations in the megakaryocyte-specific immunoreceptor tyrosine-based inhibitory motif (ITIM)-containing receptor G6b-B (*G6b*, *C6orf25* or *MPIG6B*). Patients presented with a mild-to-moderate bleeding diathesis, macrothrombocytopenia, anemia, leukocytosis and atypical megakaryocytes associated with a distinctive, focal, perimegakaryocytic pattern of bone marrow fibrosis. In addition to identifying the responsible gene, the description of G6b-B as the mutated protein potentially implicates aberrant G6b-B megakaryocytic signaling and activation in the pathogenesis of myelofibrosis. Targeted insertion of human *G6b* in mice rescued the knockout phenotype and a copy number effect of human G6b-B expression was observed. Homozygous knockin mice expressed 25% of human G6b-B and exhibited a marginal reduction in platelet count and mild alterations in platelet function; these phenotypes were more severe in heterozygous mice that expressed only 12% of human G6b-B. This study establishes G6b-B as a critical regulator of platelet homeostasis in humans and mice. In addition, the humanized *G6b* mouse will provide an invaluable tool for further investigating the physiological functions of human G6b-B as well as testing the efficacy of drugs targeting this receptor.

Introduction

Myelofibrosis in children is rare, and, in children, is most commonly seen in association with acute megakaryoblastic leukemia.[1] Other causes include acute lymphoblastic leukemia (ALL),[2] Hodgkin lymphoma[3], severe vitamin D or C deficiency,[4,5] [6] renal osteodystrophy[7], osteopetrosis, hyperparathyroidism[8], autoimmunity,[9-11] and tuberculosis.[12] The clinical, histologic and molecular features of pediatric myelofibrosis differ from primary myelofibrosis (PMF) in adults, which is typically due to somatic gain-of-function mutations in tyrosine kinase (TK) signaling pathways, including *JAK2 V617F (50%), MPL W515K/L (5-10%)* or *CALR* (35%);[13,14] TK mutations are not typically present in pediatric myelofibrosis, particularly not in young children.[15,1,16] Children with myelofibrosis have a heterogeneous phenotype with variable outcomes. Some patients have spontaneous resolution,[17,18] while others have an aggressive clinical course with progressive, sometimes fatal disease cured only by hematopoietic stem cell transplantation (HSCT)[15,19-21].

Congenital or inherited forms of myelofibrosis (cMF) are exceedingly rare with fewer than 50 cases reported.[15,18-26] Many cases occur in consanguineous families,[15,19,25] suggesting that cMF can be inherited as a autosomal recessive Mendelian trait. Genetic lesions have been identified in only a small minority of cases. In some, concurrent single lineage cytopenias have been described. For example, homozygous germline mutations in *VPS45* cause neutropenia, neutrophil dysfunction, bone marrow (BM) fibrosis, progressive marrow failure and organomegaly.[27,28] In some patients, fibrosis coexists with an intrinsic platelet disorder, such as gray platelet syndrome (GPS) to gain-of-function mutations in the Growth Factor Inhibitor 1B (*GFI1B*) gene[29] or biallelic mutations in neurobeachin-like 2 (*NBEAL2*).[30-32] These phenotypes are quite distinct from most patients with cMF.

Here we describe the clinical phenotype, distinctive histological features and biallelic loss-of-function mutations in the megakaryocyte-specific immunoreceptor tyrosine-based inhibitor motif (ITIM)-containing receptor G6b-B (*C6orf25* or *MIPG6B,* referred to as *G6b*) in four families with a clinically distinctive form of cMF associated with macrothrombocytopenia and focal myelofibrosis (cMTFM). These phenotypes closely resemble those reported in *G6b* knockout (*KO*) and loss-of-function mice (*Geer et al. co-submitted*).[33] A humanized *G6b* transgenic knockin (*KI*) mouse model establishes that human and mouse G6b-B perform orthologous functions. Mice homozygous for human *G6b* ($G6b^{hu/hu}$) exhibit a mild platelet disorder attributed to reduced human G6b-B expression. Reduced G6b-B expression in $G6b^{hu/hu}$ and heterozygous ($G6b^{hu/-}$) mice also revealed novel regulatory roles of G6b-B with respect to immunoreceptor tyrosine-based activation motif (ITAM) and hemi-ITAM receptor signaling.

Materials and Methods

Patients

Families 1-3 consented to the Pediatric Myelodysplastic Syndrome and Bone Marrow Failure Registry (Boston Children's Hospital, Protocol #10-02-0057). Family 4 was consented to the Biomedical Research Centres/Units Inherited Diseases Genetic Evaluation-Bleeding and Platelet Disorders (BRIDGE-BPD) study (UK REC10/H0304/6). All studies were conducted according to the Declaration of Helsinki.

Hematological characterization and sample preparation

Complete blood counts (CBC) and BM aspirates and biopsies were obtained on all clinically affected individuals; CBCs were obtained on other family members. Whole blood or BM mononuclear cell DNA was extracted using the Qiagen Puregene Blood Kit (Qiagen, Germantown, MD). BM aspirate and biopsy histology were prepared using standard clinical procedures. Images were obtained with an Olympus BX43 microscope and DP25 digital camera and acquired with the Olympus CellSens Entry Imaging Software.

Flow cytometry, immunohistochemistry, and immunoblotting

Flow cytometry was performed on an BD Accuri C6 flow cytometer using methods and antibodies described in the Supplemental Methods. Immunohistochemical (IHC) staining for CD61 was done on Bouin's-fixed, paraffin-embedded tissue sections using the Ventana Discovery XT automated platform. A similar, custom automated IHC method was developed using a monoclonal antibody directed against the N-terminal ectodomain of G6b-B.[33] Western blotting and immunoprecipitations were performed as previously described.[34]

Linkage and sequencing analysis

Affymetrix 6.0 SNP genotyping (QuintilesIMS, Research Triangle Park, NC) was performed on

members of the index family (Family 1) and analyzed using a custom platform (Variant Explorer, K.S.-A. and K.M., unpublished). Whole exome sequencing (WES) was performed in patients and immediate family members of Family 1 using the Illumina TrueSeq enrichment protocol. Families 2 and 3 were sequenced using the Agilent SureSelect exome capture enrichment protocol. Sequencing was performed on an Illumina Hiseq 2000/2500 with 100bp paired-end sequencing with an average depth of 40-200x (Macrogen, Rockville, MD). FASTq sequences were processed and analyzed using the WuXi/NextCode platform (Cambridge, MA). For individual 4-II-3, DNA library preparation, sequencing, variant calling and variant filtering were performed as described previously.[35] Confirmatory Sanger sequencing was carried out on all patients and available family members as described in the Supplementary Methods.

Mouse models

Humanized *G6b KI* mice were generated as outlined in Figure S1 and supplementary material (Taconic Biosciences, Cologne, Germany). *G6b* constitutive *KO* (*G6b*$^{-/-}$) mouse models were generated as previously described.[33] All mice were on a C57BL/6 background and procedures were undertaken with UK Home Office approval, in accordance with the Animals (Scientific Procedures) Act of 1986. Detailed descriptions of all other methods can be found in Supplementary Methods.

Results

Clinical and pathological characteristics

We studied four consanguineous Arab families presenting with macrothrombocytopenia, anemia and myelofibrosis. Family 1, from the United Arab Emirates (UAE), had three affected male siblings born to first cousin parents. Affected individuals (Figure 1A and Table 1, 1-III-1, 1-III-5, and 1-III-6) had macrothrombocytopenia with variably reduced platelet granularity, and microcytic anemia. BM studies revealed clusters of atypical megakaryocytes with reticulin fibrosis that was most pronounced in proximity to the megakaryocytes. Affected children had mild to moderate bleeding symptoms and required frequent platelet and occasional red cell transfusions; each affecte individual shared a homozygous human leukocyte antigen (HLA) haplotype and had congenital adrenal hyperplasia (CAH) due to 21-hydroxylase (CYP21A2) deficiency. The children had three apparently unaffected cousins born to siblings of their parents. One female cousin had CAH and shared the same homozygous HLA type as her affected cousins (Figure 1A and Table 1, 1-III-9,). She was not thrombocytopenic and had only rare large platelets on her peripheral blood smear (Figure 2C). While being evaluated as a transplant donor for her cousins, she underwent multiple BM studies, the first of which showed several lymphoid aggregates with associated reticulin, but normal megakaryocytes. Follow-up BM studies (Figure 2F, I) were normal. Given the lack of a sibling, unrelated or cord blood donor, persistent transfusion dependency and lack of response to immunomodulatory agents, patients 1-III-5 and 1-III-6 underwent successful matched related HSCTs with 1-III-9 serving as the donor. Both patients engrafted and are doing well following HSCT. The proband in this family, 1-III-1, was transplanted using a haploidentical approach from his mother, and eventually succumbed to transplant-related complications.[15]

Family 2 (Figure 1) is from Saudi Arabia. The proband (2-II-6), whose parents are first cousins, had transient thrombocytopenia at birth. Thrombocytopenia recurred at 6-months of life and was associated with severe microcytic anemia unresponsive to iron therapy. BM studies performed elsewhere at age 2-years were reported to be normal. Severe thrombocytopenia and anemia persisted despite several courses of intravenous immunoglobulin and steroids. A BM at age 3-years showed a hypercellular marrow with increased lymphocytes, and clustering of atypical megakaryocytes with focal reticulin fibrosis. The patient's older brother (2-II-5) was found to be an HLA identical match, but was ineligible as a donor due to moderate macrothrombocytopenia. BM studies are not available for this individual, though he is presumed to be clinically affected. Given the lack of a suitable donor and their mild phenotype requiring only occasional platelet transfusions, both children continue to be monitored.

The proband in Family 3 (Figure 1A, 3-II-4) is the daughter of first cousin consanguineous parents from the UAE. She presented at 15-months of age with leukocytosis, severe microcytic anemia and macrothrombocytopenia. Her clinical features were strikingly similar to the affected children in Family 1. Her BM showed a mildly hypercellular marrow for her age with a relative myeloid hyperplasia and clusters of atypical megakaryocytes with associated reticulin fibrosis. Although Family 1 and Family 3 are not known to be related, 3-II-4 also has CAH and shares the same homozygous HLA type and CYP21A2 mutation as Family 1. She is currently being followed without therapeutic intervention. *JAK2*, *MPL* and *CALR* mutation analysis was negative in patients from Fimilies 1-3 (Table 1).

The fourth family included an affected male and female sibling pair with macrothrombocytopenia, increased BM megakaryocytes, and grade II BM myelofibrosis

(Figure 1A**,** 4-II-2, 4-II-3). These children and an unaffected brother were born to first cousins of Arab descent. The affected boy (4-II-2) had a more severe phenotype, including anemia with Howell-Jolly bodies, elevated fetal hemoglobin, dyserythropoiesis and dysmegakaryopoiesis. Platelet surface expression of GPIbα, αIIb, α2 and GPIV were all unaltered, and there was a minor reduction in aggregation to ADP (*data not shown*).

A detailed description of each case is included in the Supplemental Data.

Linkage, mutational and protein expression analyses

We performed Affymetrix SNP 6.0 genotyping on peripheral blood DNA from 10 individuals from Family 1 and assessed shared regions of homozygosity by descent in 1-III-5 and 1-III-6; 1-III-9 was regarded as having an ambiguous phenotype. The major histocompatibility locus (MHC) on chromosome 6p, which, although not statistically significant, showed the strongest linkage (LOD=2.01, Figure 1B). We focused on this region, because affected individuals in Family 1 and 3 had an identical homozygous HLA type and congenital adrenal hyperplasia (CAH) due to the identical CYP21A2 mutation (Table 1). Furthermore, both affected individuals in Family 2 had a different, but homozygous, HLA haplotype; the CYP21A2 and HLA loci are located at 6p21.33 and 6p21.32-6p22.1, respectively (Figure 1B).

We performed WES on nuclear families 1-3, and on individual 4-II-3 and interrogated the results for genes in which unambiguously affected members of each family carried a homozygous rare variant (allele frequency <0.005) within the candidate disease interval predicted to be functionally deleterious. The only gene meeting these criteria was the megakaryocyte and platelet-specific receptor G6b (*MPIG6B, C6orf25*, referred to as *G6b-B* or *G6b*).

G6b-B is a transmembrane receptor expressed on the surface of platelets and megakaryocytes.[33,36-38] G6b-B has one extracellular immunoglobulin-like domain, a single transmembrane domain and an immunoreceptor tyrosine-based inhibitory motif (ITIM) and immunoreceptor tyrosine-based switch motif (ITSM) in its cytoplasmic tail. Tyrosine phosphorylation of the ITIM and ITSM provides a docking site for the SRC homology 2 (SH2) domain-containing tyrosine phosphatases SHP1 (*PTPN6*) and SHP2 (*PTPN11*), which mediate downstream signalling.[39,40] Murine KO and loss-of-function models of *G6b* result in a phenotype very similar to the patients, including macrothrombocytopenia, abnormal platelet function and the perimegakaryocytic pattern of bone marrow fibrosis present in patients (*Geer at al. co-submitted*).[33] BM-derived mouse G6b-B-deficient megakaryocytes develop and proliferate normally *in vitro*, but failed to form highly branched proplatelets, suggesting that G6b-B regulates proplatelet formation, correlating with reduced platelet production.[33]

Families 1 and 3 shared the same variant, a two base pair duplication bridging a splice donor site, NM_138272.2 c.61_61+1dup (p.?), and Family 2 had a unique homozygous frameshift mutation, c.149dup (p.Ala52GlyfsX128, Figure 1B). These variants segregated with the phenotype in families 2 and 3; however, in family 1, individual 1-III-9, who had served as the HSCT donor for her cousins, genotyped as a homozygous mutant, despite having no overt clinical features of the disease other than rare giant platelets (Figure 2C). In Family 4, we found a novel apparently homozygous missense variant c.469G>A (p.Gly157Arg, Figure 1B). The variant was also homozygous in the affected brother.

Residues 143-163 encode the predicted transmembrane domain of G6b-B, and substituting a glycine with arginine would likely destabilize insertion of the receptor into the membrane. Expression of the p.Gly157Arg mutant protein was tested using transiently transfected DT40

cells. Introduction of the mutation caused a significant reduction in total G6b-B protein expression (Figure 1C), and surface expression was reduced by 84% by flow cytometry (Figures 1D, E). A comparable reduction in expression was also observed in transiently transfected Chinese hamster ovary (CHO) cell line (*data not shown*). These data suggest that this rare missense variant is functionally significant.

To further validate *G6b* variants as disease-causing, we evaluated G6b-B expression in BM biopsy specimens from affected patients and control samples by IHC using a monoclonal antibody specific to the ectodomain. G6b-B was strongly and selectively expressed in megakaryocytes and platelets of control BM samples, but completely absent in megakaryocytes and platelets of the genotypically affected individuals from families 1-3 (Figure 2J-2O). BM biopsy samples were not available for patient 4-II-2 or 4-II-3 with the p.Gly157Arg mutation. Thus, in combination with the complementary phenotype observed in *G6b*$^{-/-}$ mice,[33] the thrombocytopenia and BM myelofibrosis found in these patients is almost certainly due to reduced or absent expression of G6b-B.

Expression of human G6b-B in *G6b*$^{hu/hu}$ mice

To confirm that human and mouse G6b-B are orthologous, we generated a humanized *G6b* mouse model in which mouse *G6b* was replaced with its human counterpart (Figure S1 and Supplemental Methods). Mice were born at expected Mendelian frequencies from heterozygous (*G6b*$^{hu/+}$) breeding pairs (Table S1), and *G6b*$^{hu/hu}$ mice were healthy, fertile and survived >25 weeks without any overt developmental or growth anomalies. Expression of human and mouse G6b-B was verified by flow cytometry (Figure S2) and western blotting (Figure 3A). Expression of the human G6b-A splice isoform, which lacks the ITIM and ITSM,

was also demonstrated using an isoform-specific antibody (Figure 3Ai, iv). Both human isoforms were only expressed at 25% of normal human platelet levels. The ratio of glycosylated (32 kDa) to unglycosylated (28 kDa) human G6b-B and -A was reduced from 3:2 in human platelets to 2:3 in *G6b*$^{hu/hu}$ platelets (Figure 3B).

The ability of human G6b-B to bind mouse Shp1 and Shp2 was also investigated in *G6b*$^{hu/hu}$ platelets (Figure 3C). Similar amounts of human and mouse Shp1 and Shp2 co-immunoprecipitated (co-IP'd) with human G6b-B from human and *G6b*$^{hu/hu}$ platelets under resting conditions (Figure 3Cii). However, less Shp1 co-IP'd with human G6b-B from *G6b*$^{hu/hu}$ platelets compared with human platelets following collagen-stimulation, most likely reflecting differences in expression levels of Shp1 and Shp2 in human and mouse platelets (Figure S3).[41,42] In contrast, comparable amounts of Shp2 co-IP'd with human G6b-B from collagen-stimulated human and *G6b*$^{hu/hu}$ platelets.

Human G6b-B functionally replaces mouse G6b-B

Reduced human G6b-B expression resulted in an 21% reduction in platelet count and a marginal increase in platelet volume in *G6b*$^{hu/hu}$ mice (Table 2, Figure S4). In contrast, complete ablation of *G6b* resulted in a >80% reduction in platelet count and >30% increase in platelet volume (Table 2), demonstrating that human G6b-B rescues the *KO* phenotype. Altered blood cell counts in *G6b KO* mice were independent of age (Figure S5). Histological sections of spleens and femurs also demonstrated that expression of human *G6b* rescues the perimegakaryocytic pattern of bone marrow fibrosis previously identified in *G6b KO* mice (Figure S6).[33] All other hematological parameters were normal in *G6b*$^{hu/hu}$ mice (Table 2).

Blood counts were normal in *G6b*$^{+/hu}$ and *G6b*$^{+/-}$ mice (Table 2).[33] Platelet surface levels of GPVI, CLEC-2, α2, αIIb and GPIbα were normal in platelets from *G6b*$^{hu/hu}$ mice (Figure S7).

Reduced human G6b-B expression causes minor alterations in platelet function

G6b$^{hu/hu}$ platelets provide a unique model to investigate the physiological consequence of reduced human G6b-B levels in platelets, without altered expression of other receptors identified in *G6b*$^{-/-}$ mice.[33] No significant defects were observed in αIIbβ3-mediated adhesion and spreading of *G6b*$^{hu/hu}$ platelets on fibrinogen, in the presence or absence of thrombin (Figure S8). Consistent with these findings, outside-in αIIbβ3 signaling was comparable between *WT* and *G6b*$^{hu/hu}$ platelets (Figure S9). Bands corresponding to tyrosine phosphorylated mouse (45 kDa) and human (28-34 kDa doublet) G6b-B were observed in fibrinogen-adhered *WT* and *G6b*$^{hu/hu}$ platelets, respectively. As *G6b*$^{hu/hu}$ mice do not express mouse G6b-B (Figure 3), the tyrosine phosphorylated band at 45 kDa is due to the presence of other co-migrating phosphorylated proteins.

We next investigated (hemi)-ITAM receptor-mediated functional responses. Unexpectedly, platelet aggregation was marginally reduced in response to low and intermediate concentrations (1-10 μg/ml) of the GPVI-specific agonist collagen-related peptide (CRP) (Figure 4A). In contrast, CLEC-2-mediated platelet aggregation was marginally increased at 6 μg/ml anti-CLEC-2 antibody (Figure 4A). Platelet aggregation to thrombin, collagen, ADP and the TxA_2 analogue U46619 were normal (Figure S10). ATP secretion from dense granules was normal to all agonists tested (Figure 4A and S10), except for a minor increase at an intermediate dose of collagen. These findings reveal minor alternations in platelet functional

responses due to reduced human G6b-B expression that are likely of no physiological consequence.

Altered *G6b*$^{hu/hu}$ platelet function does not affect thrombus formation or hemostasis

We further investigated *G6b*$^{hu/hu}$ platelet functional responses under physiological flow conditions on different thrombogenic surfaces. Platelet adhesion and thrombus formation were quantified by flowing anti-coagulated blood over: (1) collagen; (2) von Willebrand Factor-binding protein (vWF-BP) and laminin; and (3) vWF-BP, laminin and the CLEC-2 agonist rhodocytin, for 3.5 minutes at 1,000 s^{-1}. Surface area coverage and morphological scores were used as measures of platelet adhesion and thrombus formation (Figure S11). Regression analysis of a cohort of *WT* mice (n=19) did not indicate that the 21% reduction in platelet counts in *G6b*$^{hu/hu}$ mice will affect any of the measured parameters (Figure S12) The total surface area covered by *G6b*$^{hu/hu}$ platelets on collagen was unaltered compared with *WT* platelets (Figure 4B). However, multilayer thrombus formation and contraction were both significantly increased, despite a minor reduction in αIIbβ3 activation and normal α-granule release, measured by immunostaining with JON/A and P-selectin antibodies, respectively (Figure 4B). Altered thrombus morphology of *G6b*$^{hu/hu}$ platelets is most likely a reflection of the increased proportion of phosphatidylserine (PS)-positive procoagulant platelets, measured by Annexin V staining (Figure 4B).

No difference in adhesion or platelet activation were observed when anti-coagulated blood from *WT* and *G6b*$^{hu/hu}$ mice was flowed over vWF-BP and laminin, or vWF-BP, laminin and rhodocytin (Figure S13). Although some minor alterations in *G6b*$^{hu/hu}$ platelet activation were identified using this assay, expression of human G6b-B rescued the severe defects observed

in *G6b*$^{-/-}$ platelets. This rescue is likely due to a combination of increased platelet counts and normalized platelet reactivity. Functional defects observed in *G6b*$^{hu/hu}$ platelets did not culminate in compromised hemostasis in mice, as assessed using the tail bleeding assay, whereas *G6b*$^{-/-}$ mice bled excessively, as previously reported (Figure 4C).[33]

To determine the molecular basis of altered responses to CRP and anti-CLEC-2 antibody, we investigated tyrosine phosphorylation in *WT* and *G6b*$^{hu/hu}$ platelets. The findings from aggregations studies were supported by a minor reduction in global tyrosine phosphorylation following CRP stimulation (Figure 5A). A trend towards reduced SFK and Syk activities was identified, as measured by changes in autophosphorylation of Tyr418 and Tyr519/20 in the activation loops of SFKs and Syk, respectively, though this did not reach significance (Figure 5A). SFK-mediated phosphorylation of the ITAM-containing FcR γ-chain, which acts as a docking site for Syk to propagate signals downstream of GPVI, was also marginally reduced in CRP-stimulated *G6b*$^{hu/hu}$ platelets. The opposite was observed in CLEC-2 activated platelets, in which global tyrosine phosphorylation, SFK and Syk activation were marginally increased in response to antibody-mediated cross-linking and activation of CLEC-2 (Figure 5B). However, only Syk activation with 10 μg/ml anti-CLEC-2 antibody was significantly increased.

Further reduction in human G6b-B expression exacerbates platelet defects

To further investigate the threshold of human G6b-B expression required to rescue the *G6b*$^{-/-}$ phenotype, we generated human *G6b* hemizygous mice (*G6b*$^{hu/-}$) by crossing *G6b*$^{hu/hu}$ mice with *G6b*$^{-/-}$ mice (Figure 6A). *G6b*$^{hu/-}$ mice expressed only 12% of human G6b-B and -A compared with human platelets, and no mouse G6b-B (Figure 6A and S14A, B). These expression levels produced an even greater reduction in platelet counts (29%) and a

comparable increase in platelet volume (6-7%) compared with *G6b*$^{hu/hu}$ mice (Table 2). This provides further evidence that human G6b-B dose dependently regulates platelet production. Surface receptor expression was normal in *G6b*$^{hu/-}$ platelets compared with *WT* platelets, except for CLEC-2, which was marginally reduced by 16% (Figure S14C). Interestingly, platelet aggregation was further reduced in response to CRP and increased in response to antibody-mediated cross-linking of CLEC-2 (Figure 6B). These findings demonstrate differential roles of G6b-B in regulating ITAM- and hemi-ITAM-containing receptor-mediated platelet activation at these expression levels. No difference was observed upon activation of CLEC-2 using the snake toxin rhodocytin. This likely reflects the tetravalent structure of rhodocytin that can elicit a more robust CLEC-2 activating signal, thus abrogating the mild phenotype observed with the bivalent anti-CLEC-2 antibody. Thrombin-mediated aggregation of *G6b*$^{hu/-}$ platelets was normal and no significant defects in ATP secretion was observed for all agonists tested.

Discussion

Here we have described four families with a distinct phenotype of macrothrombocytopenia, microcytic anemia, variable leukocytosis and histologically characteristic megakaryocytic clustering, dysplasia and focal reticulin fibrosis in the BM presenting at young age. We attribute this to homozygous loss-of-function mutations in *G6b*, the gene encoding G6b-B, a megakaryocytic/platelet-specific ITIM-containing receptor. While this work was in preparation, another consanguineous Arab family with a similar phenotype was described with a homozygous predicted null mutation in *G6b.*[26] These data firmly support the conclusion that recessive loss-of-function mutations in *G6b* result in the phenotype that we comprehensively describe and term congenital macrothrombocytopenia with cMTFM. All of the clinically affected patients have a phenotype strikingly similar to a null mutation,[33] or mutations that abolish ITIM/ITSM signaling,(*Geer et al. co-submitted*) in the murine orthologue. Concomitantly, we have demonstrated that the *G6b KO* phenotype can be rescued upon expression of human *G6b*.

One apparently clinically unaffected individual, 1-III-9, without thrombocytopenia or anemia at the time of her evaluation as a transplant donor, also shares the G6b-B mutation; she did not have thrombocytopenia, bleeding symptoms, leukocytosis, anemia, or atypical megakaryocytes associated with fibrosis, but did have rare large platelets. She did have transient BM lymphoid aggregates that are unusual for such a young child; these might be indicators of a primary BM disorder, but could equally be due to her CAH or other causes. Thus, it is likely that even genotypically similar patients might have varying expressivity or penetrance of the phenotype due to other modifying factors, including age, environment, and genotypes at other loci. Indeed, for example, patient 2-II-5 came to medical attention only

because of his more severely affected younger sibling, 2-II-6. In addition to modifiers noted above, there are several possible explanations for the successful HSCT of the two siblings, 1-III-5 and 1-III-6 from their cousin, 1-III-9, who shares the same homozygous mutant *G6b* genotype. First, it is conceivable that the conditioning regimen alters the niche directly, which could impact the regulation of other components important in the regulation of megakaryocytic development, proplatelet and platelet formation. Second, introduction of a new hematopoietic stem cell pool from the donor into the host with cMF could lead to immunological graft and host interactions between the stem cell compartment and the niche that could alter megakaryocytic development.

The cMTFM phenotype underscores the importance of G6b-B signaling in normal megakaryocyte and platelet biology. Binding of Shp1 and Shp2 are essential for mediating signal transduced by G6b-B. A mutant form of G6b-B that uncouples it from Shp1 and Shp2 signaling phenocopies the *G6b KO* mouse model (*Geer et al. co-submitted*),[33] and a tissue-specific mouse model of combined Shp1 and Shp2 deficiency recapitulates multiple features of *G6b KO* animals,[43] further indicating the essential nature of this signaling pathway to megakaryocyte function.

The majority of reported patients with cMF have undergone HSCT as it was felt to be the only curative treatment optio.[15] The histological resemblance to PMF in adults, which carries a risk of evolution to acute myeloid leukemia and a poor prognosis, may have encouraged providers to offer HSCT out of due caution, even in the absence of evidence for adverse outcomes when managed conservatively. Indeed, in our series of 7 cases of patients with *G6b* mutations, three required HSCT for cytopenias, one was clinically unaffected, and three have been observed without ongoing clinical interventions. The identification of a molecular therapeutic

target—Shp1- and Shp2-dependent signal transduction—now offers the potential to circumvent the G6b-B deficiency in cMTFM and insights into the pathogenesis of other forms of primary and secondary myelofibrosis.

The humanized *G6b* mouse provided compelling evidence of the analogous functions of human and mouse G6b-B. The mild platelet phenotype, suggests human G6b-B interacts with the same ligands and signals in a similar manner to mouse G6b-B. Reduced binding of human G6b-B to mouse Shp1 is most likely a reflection of the relative stoichiometries and binding affinities of Shp1 and Shp2 in mouse platelets. Mouse platelets contain 6-fold higher levels of Shp2 than Shp1, whereas human platelets contain 2-fold more Shp1 than Shp2 (Figure S3).[41,42] In addition, the binding affinity of tandem SH2 domains of human Shp2 with phosphorylated-G6b-B-ITIM-ITSM peptide is 100-fold greater than the binding affinity of tandem SH2 domains of Shp1.[44] However, differences in the proportions of human G6b-B bound Shp1 and Shp2 in mouse versus human platelets are not likely to underlie the platelet defects described the humanized *G6b* mouse, as mouse G6b-B is predicted to bind the same ratios of Shp1 and Shp2. Thus, platelet defects are more likely due to reduced human G6b-B expression.

Despite the significant reduction in human G6b-B in *G6b*$^{hu/hu}$ and *G6b*$^{hu/-}$ mice, both mouse models exhibited only mild platelet phenotypes. A large proportion of G6b-B is therefore not essential for maintenance of platelet homeostasis. MKs from *G6b*$^{-/-}$ mice were previously shown to develop normally *in vitro*, but with significantly diminished proplatelet production capacity.[33] Reduced platelet production in *G6b*$^{hu/hu}$ and *G6b*$^{hu/-}$ mice could therefore have been as a consequence of aberrant proplatelet formation, arising from reduced G6b-B expression in MKs. The dose dependent nature of the reduction in platelet counts in these

homozygous and heterozygous mice adds to the growing body of evidence of the vital role of G6b-B in regulating platelet production.

The reduction in human G6b-B expression was predicted to lead to an increase in platelet reactivity to collagen. Indeed, thrombus formation and contraction were significantly increased when whole blood was flowed over collagen, despite a marginal reduction in integrin αIIbβ3 activation. This can be explained by an enhancement in PS exposure and increased procoagulant activity of *G6b*$^{hu/hu}$ platelets, which is dependent upon PLCγ2-mediated Ca^{2+} flux and phosphatidylinositol 3-kinase signaling,[45] highlighting these as potential downstream targets of Shp1 and Shp2. The dose-dependent reduction in aggregation of *G6b*$^{hu/hu}$ and *G6b*$^{hu/-}$ platelets to CRP was however, counter-intuitive, suggesting G6b-B may act as both a positive and negative regulator of GPVI signaling, depending upon expression levels. The candidate target of G6b-B-associated Shp1 and Shp2 is Syk tyrosine kinase that we previously showed is hyper-activated in G6b-B-deficient platelets.[33] Syk contains multiple regulatory tyrosine phosphorylation sites that Shp1 and Shp2 may differentially dephosphorylate, depending upon the expression level of G6b-B, leading to either positive or negative effects on Syk activity.[46]

This study establishes that human and mouse G6b-B perform the same physiological functions, and that deletion and loss-of-function mutations in G6b-B lead to megakaryocytic and myelofibrotic disorders in both species. Validation of these analogous functions is essential to progress with exploring the role of G6b-B in various pathological conditions in humans and as a novel therapeutic drug target. The humanized G6b-B mouse model described here provides an invaluable tool for investigating the efficacy and therapeutic potential of agents targeting human G6b-B in various disease conditions, including

myeloproliferation and myelofibrosis, allowing for a greater understanding of the mechanism of action of these therapies.

Acknowledgements

Sample collection and clinical and pathology analysis was performed under the Pediatric MDS and BMF Registry supported by NIH grant R24 DK 099808. I.H. and M.D.F. are supported by R24 DK099808. M.J.G. is funded by a Medical Research Council PhD studentship (GBT1564), A.M. is a BHF Intermediate Basic Science Research Fellow (FS/15/58/31784) and Y.A.S. is a BHF Senior Basic Science Research Fellow (FS/13/1/29894). T.V. was funded by the Deutsche Forschungsgemeinschaft (DFG V2134-1/1).

Authorship Contributions

I.H. – identified patients, analyzed the clinical and pathologic phenotypes, designed the study, wrote and revised the manuscript

M.J.G. – performed experiments, analyzed data, wrote and revised the manuscript

T.V. – performed experiments, analyzed data, revised the manuscript

A.C. – performed patient sample processing and sequencing analysis

D.R.C. – performed patient sample processing and sequencing analysis

A.B. – performed experiments, analyzed data

M.L.C. – developed the customized immunohistochemistry for G6b-B

S.H. – performed experiments, analyzed data

J.P.V.G. – performed experiments, analyzed data, revised the manuscript

M.J.E.K. – performed experiments, analyzed data

J.W.M.H. – performed experiments, analyzed data

J.A.E. – provided snake toxin rhodocytin

K.S.A. – performed linkage and WES data analysis

E.A.O. – provided patient care

M.D. – performed experiments, analyzed data

K.F. – performed GWAS

C.P. – identified and diagnosed patient

R.F. – identified and diagnosed patient

G.E.J. – analyzed data, revised the manuscript

K.M. – performed linkage and WES data analysis

E.T. –analyzed data, revised the manuscript

W.H.O. – analyzed data, contributed intellectually

A.M. – designed experiments, analyzed data, revised the manuscript

M.D.F. – analyzed the clinical and pathologic phenotypes, designed the study, wrote and revised the manuscript

Y.A.S. – conceptualized, designed experiments, analyzed data, wrote and revised the manuscript

All authors contributed to the revision of the manuscript.

Disclosure of Conflicts of Interest

The authors have no competing financial interests to declare.

References

1. Hofmann I. Myeloproliferative Neoplasms in Children. *J Hematop*. 2015;8(3):143-157.
2. Hann IM, Evans DI, Marsden HB, Jones PM, Palmer MK. Bone marrow fibrosis in acute lymphoblastic leukaemia of childhood. *J Clin Pathol*. 1978;31(4):313-315.
3. Carroll WL, Berberich FR, Glader BE. Pancytopenia with myelofibrosis. An unusual presentation of childhood Hodgkin's disease. *Clin Pediatr (Phila)*. 1986;25(2):106-108.
4. Balkan C, Ersoy B, Nese N. Myelofibrosis associated with severe vitamin D deficiency rickets. *J Int Med Res*. 2005;33(3):356-359.
5. al-Eissa YA, al-Mashhadani SA. Myelofibrosis in severe combined immunodeficiency due to vitamin D deficiency rickets. *Acta Haematol*. 1994;92(3):160-163.
6. Fain O, Mathieu E, Thomas M. Scurvy in patients with cancer. *BMJ*. 1998;316(7145):1661-1662.
7. Schlackman N, Green AA, Naiman JL. Myelofibrosis in children with chronic renal insufficiency. *J Pediatr*. 1975;87(5):720-724.
8. Kumbasar B, Taylan I, Kazancioglu R, Agan M, Yenigun M, Sar F. Myelofibrosis secondary to hyperparathyroidism. *Exp Clin Endocrinol Diabetes*. 2004;112(3):127-130.
9. Phebus CK, Penchansky L. Autoimmune pancytopenia progressing to acute myelofibrosis. *Scand J Haematol*. 1986;36(3):317-318.
10. Passamonti F, Rumi E, Arcaini L, et al. Prognostic factors for thrombosis, myelofibrosis, and leukemia in essential thrombocythemia: a study of 605 patients. *Haematologica*. 2008;93(11):1645-1651.
11. Paquette RL, Meshkinpour A, Rosen PJ. Autoimmune myelofibrosis. A steroid-responsive cause of bone marrow fibrosis associated with systemic lupus erythematosus. *Medicine (Baltimore)*. 1994;73(3):145-152.
12. Hashim MS, Kordofani AY, el Dabi MA. Tuberculosis and myelofibrosis in children: a report. *Ann Trop Paediatr*. 1997;17(1):61-65.
13. Nangalia J, Massie CE, Baxter EJ, et al. Somatic CALR mutations in myeloproliferative neoplasms with nonmutated JAK2. *N Engl J Med*. 2013;369(25):2391-2405.
14. Klampfl T, Gisslinger H, Harutyunyan AS, et al. Somatic mutations of calreticulin in myeloproliferative neoplasms. *N Engl J Med*. 2013;369(25):2379-2390.
15. DeLario MR, Sheehan AM, Ataya R, et al. Clinical, histopathologic, and genetic features of pediatric primary myelofibrosis--an entity different from adults. *Am J Hematol*. 2012;87(5):461-464.
16. An W, Wan Y, Guo Y, et al. CALR mutation screening in pediatric primary myelofibrosis. *Pediatr Blood Cancer*. 2014;61(12):2256-2262.
17. Lau SO, Ramsay NK, Smith CM, 2nd, McKenna R, Kersey JH. Spontaneous resolution of severe childhood myelofibrosis. *J Pediatr*. 1981;98(4):585-588.
18. Altura RA, Head DR, Wang WC. Long-term survival of infants with idiopathic myelofibrosis. *Br J Haematol*. 2000;109(2):459-462.
19. Sieff CA, Malleson P. Familial myelofibrosis. *Arch Dis Child*. 1980;55(11):888-893.
20. Sekhar M, Prentice HG, Popat U, et al. Idiopathic myelofibrosis in children. *Br J Haematol*. 1996;93(2):394-397.
21. Domm J, Calder C, Manes B, Crossno C, Correa H, Frangoul H. Unrelated stem cell transplant for infantile idiopathic myelofibrosis. *Pediatr Blood Cancer*. 2009;52(7):893-895.
22. Boxer LA, Camitta BM, Berenberg W, Fanning JP. Myelofibrosis-myeloid metaplasia in childhood. *Pediatrics*. 1975;55(6):861-865.
23. Mallouh AA, Sa'di AR. Agnogenic myeloid metaplasia in children. *Am J Dis Child*. 1992;146(8):965-967.
24. Sah A, Minford A, Parapia LA. Spontaneous remission of juvenile idiopathic myelofibrosis. *Br J Haematol*. 2001;112(4):1083.
25. Sheikha A. Fatal familial infantile myelofibrosis. *J Pediatr Hematol Oncol*. 2004;26(3):164-168.
26. Melhem M, Abu-Farha M, Antony D, et al. Novel G6B gene variant causes familial autosomal recessive thrombocytopenia and anemia. *Eur J Haematol*. 2017;98(3):218-227.
27. Stepensky P, Saada A, Cowan M, et al. The Thr224Asn mutation in the VPS45 gene is associated with the congenital neutropenia and primary myelofibrosis of infancy. *Blood*. 2013;121(25):5078-5087.
28. Vilboux T, Lev A, Malicdan MC, et al. A congenital neutrophil defect syndrome associated with mutations in VPS45. *N Engl J Med*. 2013;369(1):54-65.
29. Monteferrario D, Bolar NA, Marneth AE, et al. A dominant-negative GFI1B mutation in the gray platelet syndrome. *N Engl J Med*. 2014;370(3):245-253.

30. Albers CA, Cvejic A, Favier R, et al. Exome sequencing identifies NBEAL2 as the causative gene for gray platelet syndrome. *Nat Genet*. 2011;43(8):735-737.
31. Gunay-Aygun M, Falik-Zaccai TC, Vilboux T, et al. NBEAL2 is mutated in gray platelet syndrome and is required for biogenesis of platelet alpha-granules. *Nat Genet*. 2011;43(8):732-734.
32. Kahr WH, Hinckley J, Li L, et al. Mutations in NBEAL2, encoding a BEACH protein, cause gray platelet syndrome. *Nat Genet*. 2011;43(8):738-740.
33. Mazharian A, Wang YJ, Mori J, et al. Mice lacking the ITIM-containing receptor G6b-B exhibit macrothrombocytopenia and aberrant platelet function. *Sci Signal*. 2012;5(248):ra78.
34. Pearce AC, Senis YA, Billadeau DD, Turner M, Watson SP, Vigorito E. Vav1 and vav3 have critical but redundant roles in mediating platelet activation by collagen. *J Biol Chem*. 2004;279(52):53955-53962.
35. Westbury SK, Turro E, Greene D, et al. Human phenotype ontology annotation and cluster analysis to unravel genetic defects in 707 cases with unexplained bleeding and platelet disorders. *Genome Med*. 2015;7(1):36.
36. Lewandrowski U, Wortelkamp S, Lohrig K, et al. Platelet membrane proteomics: a novel repository for functional research. *Blood*. 2009;114(1):e10-19.
37. Macaulay IC, Tijssen MR, Thijssen-Timmer DC, et al. Comparative gene expression profiling of in vitro differentiated megakaryocytes and erythroblasts identifies novel activatory and inhibitory platelet membrane proteins. *Blood*. 2007;109(8):3260-3269.
38. Senis YA, Tomlinson MG, Garcia A, et al. A comprehensive proteomics and genomics analysis reveals novel transmembrane proteins in human platelets and mouse megakaryocytes including G6b-B, a novel immunoreceptor tyrosine-based inhibitory motif protein. *Mol Cell Proteomics*. 2007;6(3):548-564.
39. Daeron M, Jaeger S, Du Pasquier L, Vivier E. Immunoreceptor tyrosine-based inhibition motifs: a quest in the past and future. *Immunol Rev*. 2008;224:11-43.
40. Coxon CH, Geer MJ, Senis YA. ITIM receptors: more than just inhibitors of platelet activation. *Blood*. 2017;129(26):3407-3418.
41. Burkhart JM, Vaudel M, Gambaryan S, et al. The first comprehensive and quantitative analysis of human platelet protein composition allows the comparative analysis of structural and functional pathways. *Blood*. 2012;120(15):e73-82.
42. Zeiler M, Moser M, Mann M. Copy number analysis of the murine platelet proteome spanning the complete abundance range. *Mol Cell Proteomics*. 2014;13(12):3435-3445.
43. Mazharian A, Mori J, Wang YJ, et al. Megakaryocyte-specific deletion of the protein-tyrosine phosphatases Shp1 and Shp2 causes abnormal megakaryocyte development, platelet production, and function. *Blood*. 2013;121(20):4205-4220.
44. Coxon CH, Sadler AJ, Huo J, Campbell RD. An investigation of hierachical protein recruitment to the inhibitory platelet receptor, G6B-b. *PLoS One*. 2012;7(11):e49543.
45. Munnix IC, Cosemans JM, Auger JM, Heemskerk JW. Platelet response heterogeneity in thrombus formation. *Thromb Haemost*. 2009;102(6):1149-1156.
46. Mocsai A, Ruland J, Tybulewicz VL. The SYK tyrosine kinase: a crucial player in diverse biological functions. *Nat Rev Immunol*. 2010;10(6):387-402.
47. McCarty OJ, Larson MK, Auger JM, et al. Rac1 is essential for platelet lamellipodia formation and aggregate stability under flow. *J Biol Chem*. 2005;280(47):39474-39484.
48. Senis YA, Tomlinson MG, Ellison S, et al. The tyrosine phosphatase CD148 is an essential positive regulator of platelet activation and thrombosis. *Blood*. 2009;113(20):4942-4954.
49. Ohlmann P, Eckly A, Freund M, Cazenave JP, Offermanns S, Gachet C. ADP induces partial platelet aggregation without shape change and potentiates collagen-induced aggregation in the absence of Galphaq. *Blood*. 2000;96(6):2134-2139.
50. de Witt SM, Swieringa F, Cavill R, et al. Identification of platelet function defects by multi-parameter assessment of thrombus formation. *Nature Communications*. 2014;5.

Tables

Table 1. Clinical and laboratory characteristics, treatments and outcomes of patients with congenital myelofibrosis.

1-III-1	5 m	M	NA	6.0	20	66.0	NA	microcytosis, anisopoikilocytosis, target cells, ovalocytes, large platelets	CAH	Neg	ND	ND	no pre-HSCT therapy S/P 2 haploidentical HSCT from mother	11:01 11:01	41:01 41:01	07:01 07:01	08:04 08:04	03:01 03:01	c.61_61+1dup/ c.61_61+1dup	Deceased from SCT complications, graft failure after 2nd HSCT, GI bleed, ARDS
1-III-5	Birth	M	NA	6.9	16	NA	NA	anisopoikilocytosis, target cells, basophilic stippling, large platelets	CAH	Neg	Neg	Neg	steroids, transient partial response but not sustained. Platelets declined with taper. MRD HSCT from 1-III-9	11:01 11:01	41:01 41:01	07:01 07:01	08:04 08:04	03:01 03:01	c.61_61+1dup/ c.61_61+1dup	6 years post-HSCT, engrafted, maturing trilineage hematopoiesis with no evidence of fibrosis.
1-III-6	6 m	M	13.79	8.7	19	68.0	NA	microcytosis, anisopoikilocytosis, target cells, basophilic stippling, tear drops, frequent large platelets	CAH	Neg	Neg	Neg	no pre-HSCT therapy. MRD HSCT from 1-III-9	11:01 11:01	41:01 41:01	07:01 07:01	08:04 08:04	03:01 03:01	c.61_61+1dup/ c.61_61+1dup	4 years post-HSCT. Slow platelet and RBC engraftment. Maturing trilineage hematopoiesis and no evidence of fibrosis, but platelets remain decreased, ~119-142 x10^9/L.
1-III-9	2 y	F	8.39	11.9	468	72.0	8.2	microcytosis	CAH, mild iron deficiency	ND	ND	ND	none	11:01 11:01	41:01 41:01	07:01 07:01	08:04 08:04	03:01 03:01	c.61_61+1dup/ c.61_61+1dup	Clinically unaffected, rare giant platelets
2-II-5	7 y	M	5.43	11.7	107	80.5	NA	anisopoikilocytosis, microcytosis, ovalocytes, burr cells, helmet cells, acanthocytes, schistocytes, frequent large platelets	None	ND	ND	ND	none	23:01 23:01	50:01 50:01	06:02 06:02	04:06 04:06	04:02 04:02	c.147insT p.Ala52GlyfsX128	Observation, stable disease
2-II-6	6 m	M	NA	5.4	10	65.0	12-24	anisopoikilocytosis, microcytosis, elliptocytes, schistocytes, frequent large platelets	None	Neg	Neg	Neg	IVIG x1 Steroids x1 with transient responses	23:01 23:01	50:01 50:01	06:02 06:02	04:06 04:06	04:02 04:02	c.147insT p.Ala52GlyfsX128	Observation, stable disease
3-II-4	17 m	F	19.2	5.1	81	71.3	NA	anisopoikilocytosis, microcytosis, target cells, ovalocytes, burr cells, tear drop cells, schistocytes, frequent large platelets	CAH, asplenia	Neg	Neg	Neg	none	11:01 11:01	41:01 41:01	07:01 07:01	08:04 08:04	03:01 03:01	c.61_61+1dup/ c.61_61+1dup	Observation, stable disease
4-II-2	18 m	M	NA	5.4	96	NA	NA	Anisopoikylocytosis, target cells, schistocytes, leptocytes, dacryocytes, Howell-Jolly bodies	cerebral cavernoma	ND	Neg	ND	IVIG and steroid, no response	ND	ND	ND	ND	ND	c.469G>A p.Gly157Arg	Observation, stable thrombocytopenia, supportive care with platelets
4-II-3	1 y	F	17	12.5	97	NA	NA	Anisopoikylocytosis, target cells, schistocytes, leptocytes, dacryocytes, Howell-Jolly bodies	None	ND	ND	ND	none	ND	ND	ND	ND	ND	c.469G>A p.Gly157Arg	Observation, stable mild/moderate thrombocytopenia

not available (NA), not done (ND), congenital adrenal hyperplasia (CAH), hematopoietic stem cell transplant (HSCT)

Table 2. Peripheral blood counts of indicated mouse genotypes

Hematological parameters	*WT* n=36	*G6b*$^{+/hu}$ n=37	*G6b*$^{hu/hu}$ n=37	*G6b*$^{hu/-}$ n=31	*G6b*$^{-/-}$ n=37	*λ*	*P*
Platelets (10^9/L)	1118 ± 209	1127 ± 219	884 ± 214***	795 ± 187***	206 ± 86***	0.2	2×10^{-72}
Mean platelet volume (fl)	5.8 ± 0.2	5.8 ± 0.2	6.1 ± 0.5***	6.2 ± 0.4***	7.8 ± 0.4***	-2	2×10^{-65}
Plateletcrit (%)	0.4 ± 0.1	0.4 ± 0.1	0.3 ± 0.1	0.3 ± 0.1	0.1 ± 0	-	-
Red blood cells (10^{12}/L)	11.1 ± 0.7	10.5 ± 0.7	10.7 ± 0.8	10.4 ± 0.6	10.0 ± 0.6	-	-
Hematocrit (%)	33.6 ± 2.4	32.7 ± 1.8	33.1 ± 2.5	34.1 ± 1.9	31.8 ± 1.7	-	-
White blood cells (10^9/L)	7.5 ± 3.6	8.6 ± 2.3	7.4 ± 2.6	10.1 ± 6.1	13.1 ± 6.8***	0.5	8×10^{-7}
Lymphocytes (10^9/L)	6.2 ± 2.7	7.4 ± 2.0	6.9 ± 2.2	7.8 ± 3.7	11.8 ± 4.9***	0.5	3×10^{-11}
Monocytes (10^9/L)	0.5 ± 0.4	0.3 ± 0.2	0.5 ± 0.2	0.3 ± 0.3	0.5 ± 0.4	-	-
Neutrophils (10^9/L)	0.8 ± 0.4	0.9 ± 0.4	0.7 ± 0.3	1.2 ± 0.8	1.7 ± 1.1	-	-
Eosinophils (10^9/L)	0.1 ± 0.2	0 ± 0	0 ± 0	0 ± 0.1	0 ± 0	-	-
Basophils (10^9/L)	0.1 ± 0.3	0 ± 0	0.1 ± 0.2	0 ± 0.1	0.1 ± 0.1	-	-

All values expressed as mean ± SD.
λ is the coefficient for the power transformation to minimize heteroscedasticity and non-normality
P is the result of a one-way ANOVA on transformed data
*** indicates P < 0.001 compared to *WT* with Dunnett's post hoc test

Figure legends

Figure 1. cMTFM is due to mutations in G6b-B (*G6b)*. (A) Family pedigrees. Black arrows point to the probands in each family. Double line indicates a consanguineous relationship. Ages are provided at the time of the initial evaluation of the youngest affected individual in the family. For the deceased proband the age at diagnosis and age of death is listed. (B) Ideograms showing cMTFM linkage region, the *G6b* (*MPIG6B*) locus and patient mutations. (C) Expression of p.Gly157Arg mutant in DT40 cells leads to (C) protein instability and (D, E) reduced expression on the surface of the cell (mean ± SEM, n=2). pcDNA3 vector, grey; *G6b-B WT*, green; *G6b-B p.Gly157Arg*, red, MFI, median fluorescence intensity, representative blots and histograms of two independent experiments.

Figure 2. Pathology of cMTFM. Wright-Giemsa stained peripheral blood smears from (A) a normal control, (B) patient 3-II-4 and (C) the clinically unaffected, genotypically *G6b*-mutated individual 1-III-9. Note the large, hypogranular platelets (arrow) and RBC anisocytosis in 3-II-4 and the rare giant platelet in 1-III-9 (arrow). Serial histologic sections of a bone marrow biopsies from (D, G, J, M) a normal control individual, (E, H, K, N) 3-II-4, and (F, I, L, O) 1-III-9 stained with (D-F) H&E, (G-I) Reticulin, (J-L) the megakaryocytic marker CD61, and (M-O) G6b-B. Atypical megakaryocytes present in stellate clusters associated with increased reticulin staining are characteristic of cMTMF. Staining for G6b-B is entirely negative in the megakaryocytes and platelets from 3-II-4 and 1-III-9.

Figure 3. Expression of *G6b* isoforms in humanized mouse model. (A) *WT, G6b*$^{hu/+}$, *G6b*$^{hu/hu}$, human and *G6b*$^{-/-}$ washed platelet lysates (4×10^8/mL), were resolved by SDS-PAGE and custom antibodies used to detect mouse (m)G6b-B, human (h)G6b-B and hG6b-A. Expression was quantified and normalized to (i) *WT* or (ii, iii) human lysates, to show relevant

expression levels in the mouse models. (B) Quantification of glycosylated and unglycosylated human G6b-A and -B, data normalized to show percentage of total expression. (C) hG6b-B was immunoprecipitated (IP) from basal and collagen activated *G6b*$^{hu/hu}$ and human washed platelet lysates (4 × 10^8/mL). Co-IP of Shp1 and Shp2 was investigated by (i) SDS-PAGE before (ii) quantification and normalization to hG6b-B levels. Quantification was completed using Licor Odyssey system. All data represented as mean ± SEM (n=3-4), *** *P*<0.001.

Figure 4. Minor alterations of *G6b*$^{hu/hu}$ platelet functional responses. (A) Averaged aggregation and ATP release traces for washed platelets (2 × 10^8/mL) activated with indicated concentrations of CRP and anti-CLEC-2 antibody (Ab). Area under the curve (AUC) quantification of (iii) platelet aggregation and (iv) ATP release (n=5-6 per condition, ** *P*<0.005 and * *P*<0.05). (B) Heparin-PPACK-fragmin anti-coagulated whole blood was flowed over glass coverslips coated with collagen immediately following collection. (i) Brightfield images were immediately collected, followed by staining with PE-conjugated JON/A, FITC-conjugated P-selectin and Alexa647-conjugated Annexin V and fluorescence imaging. Analysis quantifying (ii-vi) thrombus surface area coverage and morphological scores of adhered platelets, (n=5-6, *** *P*<0.001, ** *P*<0.005) and (vii-ix) surface area coverage of fluorescently labeled antibodies (n=5-6, *** *P*<0.001, * *P*<0.05). (C) Total blood loss to body weight ratio of mice following excision of tail tip (n=12-16, *** *P*<0.001, ** *P*<0.005). All data collection and analysis in panels B and C were completed blinded, mean ± SEM, scale bar: 10 μm

Figure 5. Altered tyrosine phosphorylation in response to GPVI and CLEC-2 agonists in *G6b*$^{hu/hu}$ platelets. Representative blots (n=3) of lysates prepared from washed platelets (4 × 10^8/mL) activated with indicated concentrations of (A) CRP (90 s, 10 μM lotrafiban, 10 μM indomethacin and 2 U/ml apyrase) or (B) CLEC-2 Ab (300 s, 10 μM lotrafiban) and probed with

the indicated antibodies. Src family kinase (SFK) phosphotyrosine (pTyr)418 and Syk pTyr519/20 were quantified using ImageJ and normalized to total tubulin and Syk reblots, respectively.

Figure 6. Further reduction in hG6b-B expression exacerbates observed phenotype. (A) *G6b*$^{hu/hu}$ mice were crossed with *G6b*$^{-/-}$ mice to produce hemizygous (*G6b*$^{hu/-}$) mice. (ii) Representative blots and (iii) quantification of hG6b-B expression in the indicated genotypes (n=3). (B) Average aggregation and ATP release traces and quantification of area under the curve (AUC) investigating functional response of *G6b*$^{hu/-}$ mouse washed platelets (2×10^8/mL) in response to indicated agonists (n=5-6, *** $P<0.001$, * $P<0.05$). All bar graphs presented as mean ± SEM.

Figure 1

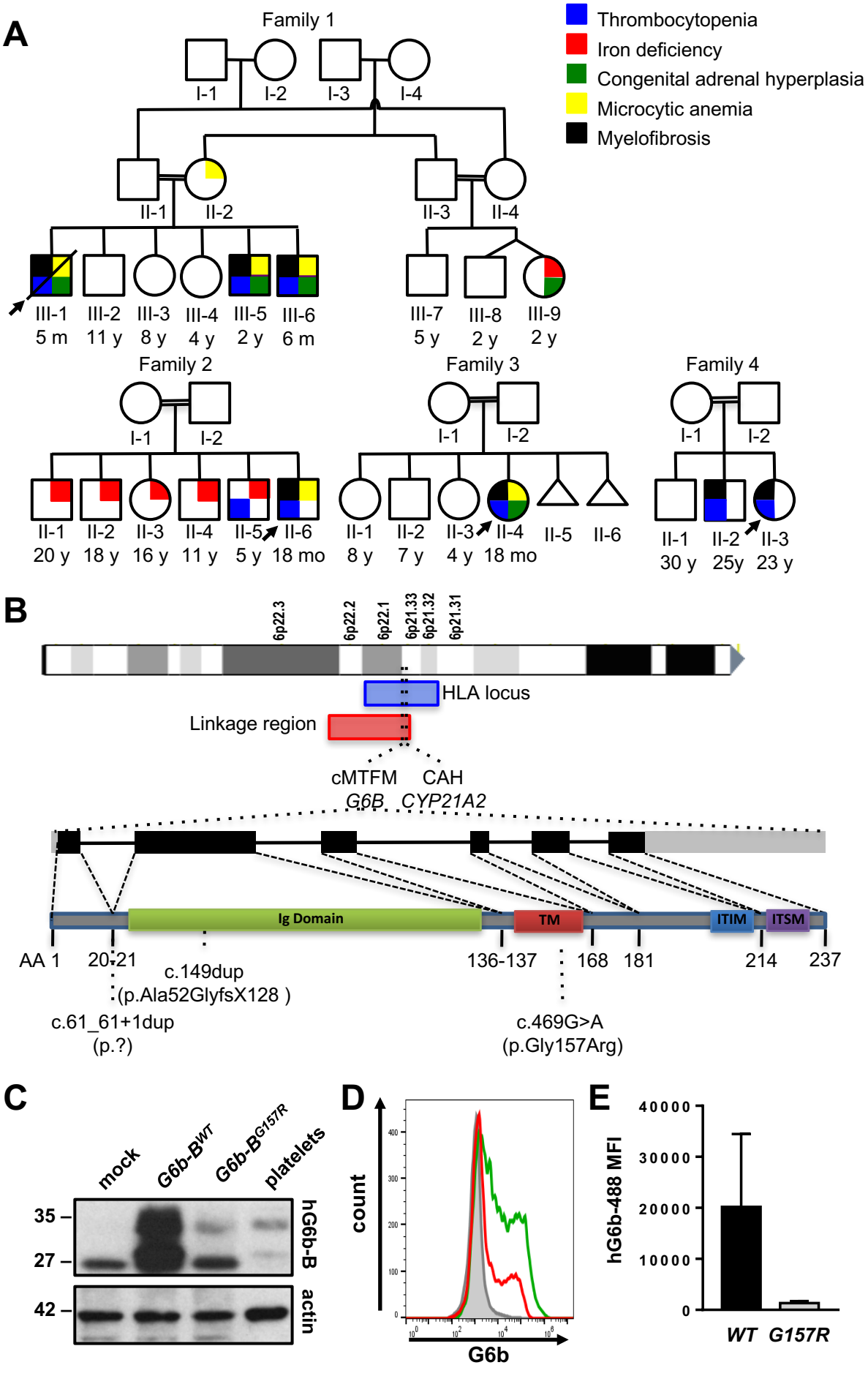
A
Family 1
Thrombocytopenia
Iron deficiency
Congenital adrenal hyperplasia
Microcytic anemia
Myelofibrosis
I-1 I-2 I-3 I-4
II-1 II-2 II-3 II-4
III-1 5 m
III-2 11 y
III-3 8 y
III-4 4 y
III-5 2 y
III-6 6 m
III-7 5 y
III-8 2 y
III-9 2 y
Family 2
I-1 I-2
II-1 20 y
II-2 18 y
II-3 16 y
II-4 11 y
II-5 5 y
II-6 18 mo
Family 3
I-1 I-2
II-1 8 y
II-2 7 y
II-3 4 y
II-4 18 mo
II-5
II-6
Family 4
I-1 I-2
II-1 30 y
II-2 25y
II-3 23 y
B
6p22.3
6p22.2
6p22.1
6p21.33
6p21.32
6p21.31
HLA locus
Linkage region
cMTFM
CAH
G6B
CYP21A2
Ig Domain
TM
ITIM
ITSM
AA 1
20-21
c.149dup
(p.Ala52GlyfsX128)
c.61_61+1dup
(p.?)
136-137
168
181
214
237
c.469G>A
(p.Gly157Arg)
C
mock
G6b-B^WT
G6b-B^G157R
platelets
35
27
42
hG6b-B
actin
D
count
G6b
E
hG6b-488 MFI
40000
30000
20000
10000
0
WT
G157R

Figure 2

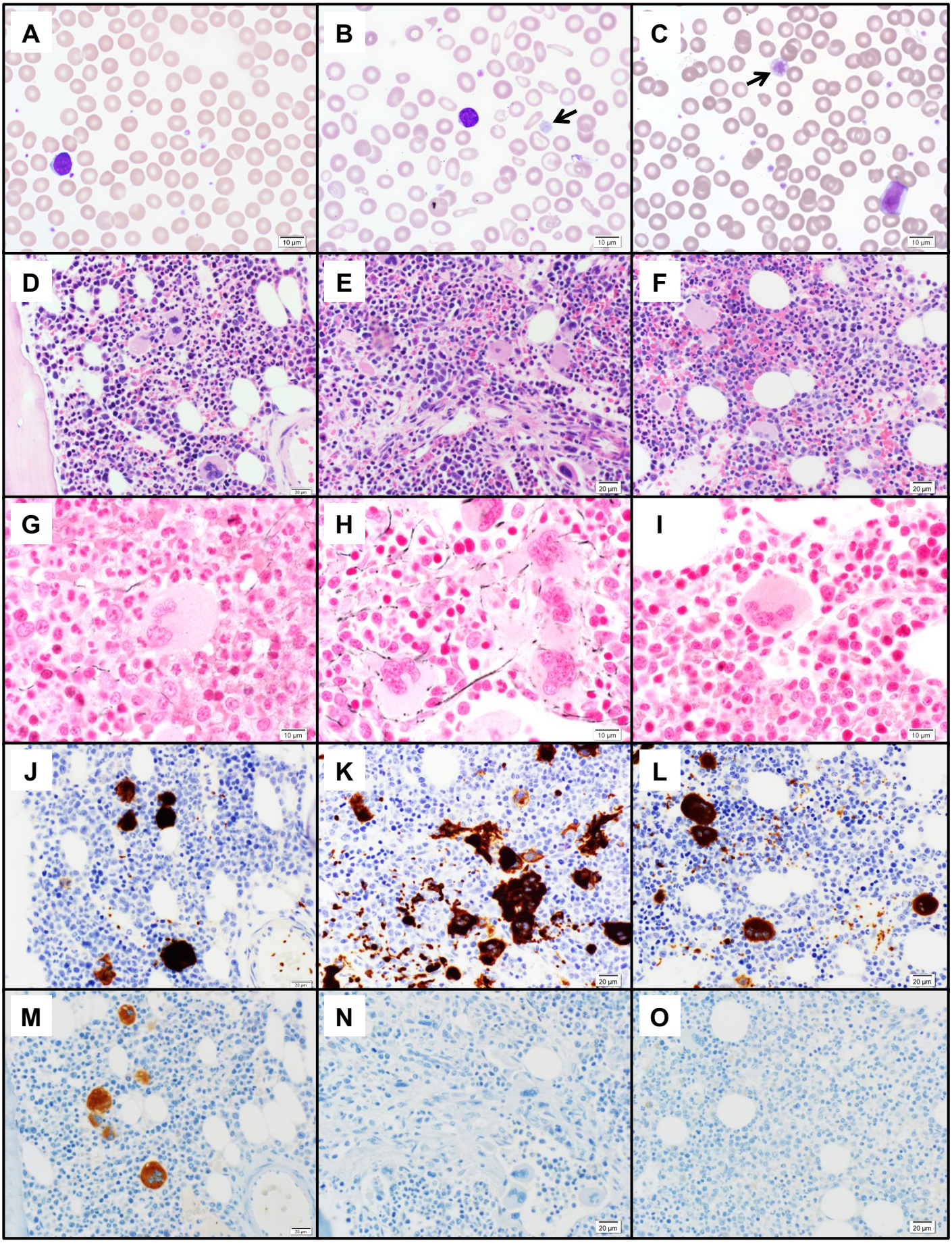

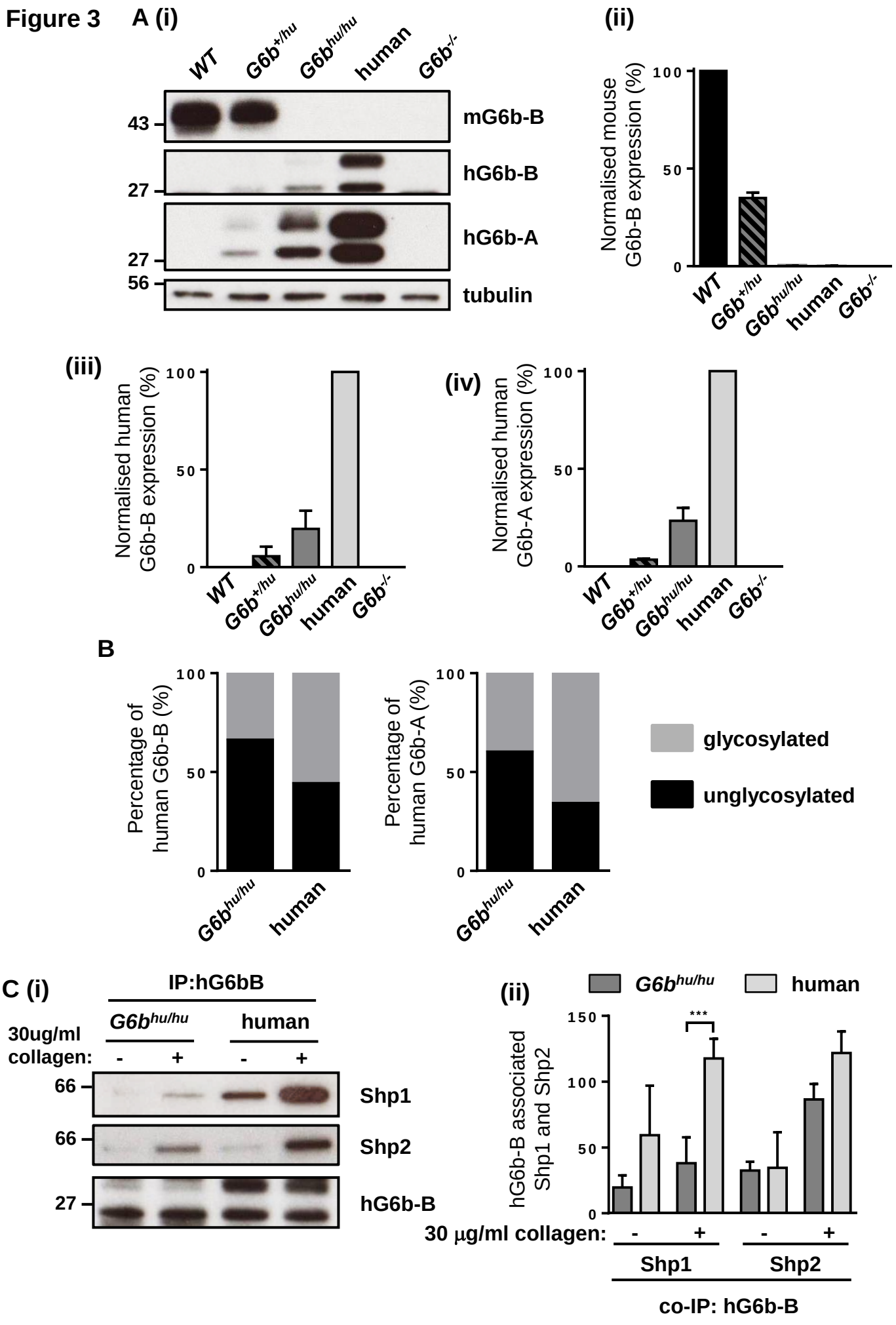
Figure 3
A (i)
WT
G6b+/hu
G6bhu/hu
human
G6b-/-
43
27
27
56
mG6b-B
hG6b-B
hG6b-A
tubulin
(ii)
Normalised mouse G6b-B expression (%)
100
50
0
(iii)
Normalised human G6b-B expression (%)
(iv)
Normalised human G6b-A expression (%)
B
Percentage of human G6b-B (%)
Percentage of human G6b-A (%)
glycosylated
unglycosylated
C (i)
IP:hG6bB
30ug/ml collagen:
- + - +
66
66
27
Shp1
Shp2
hG6b-B
(ii)
hG6b-B associated Shp1 and Shp2
150
***
30 μg/ml collagen:
Shp1
Shp2
co-IP: hG6b-B

Figure 4

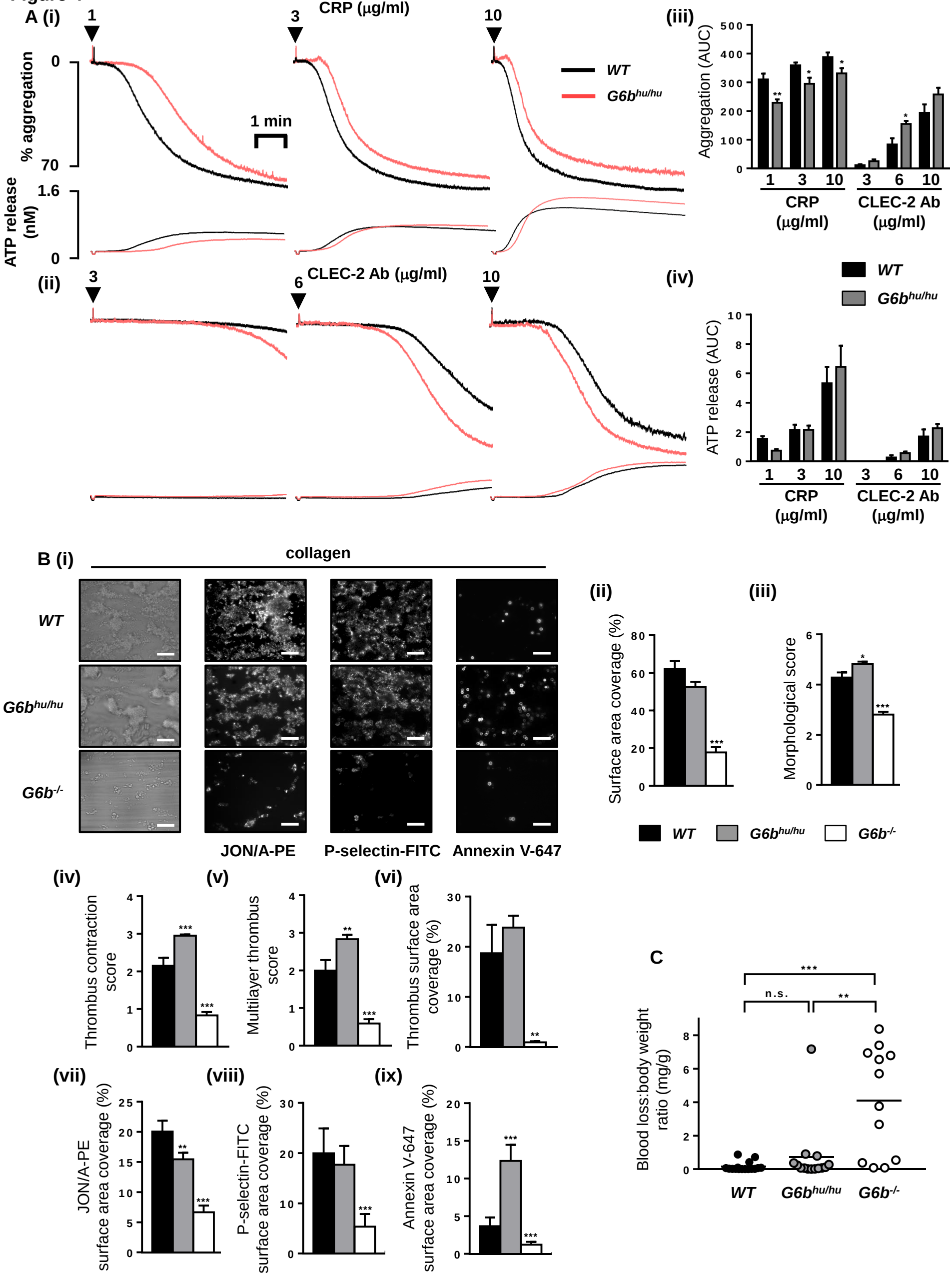
A (i)
CRP (μg/ml)
1
3
10
% aggregation
0
70
1 min
ATP release (nM)
1.6
0
WT
G6b hu/hu
(ii)
CLEC-2 Ab (μg/ml)
3
6
10
(iii)
Aggregation (AUC)
500
400
300
200
100
0
1 3 10
CRP (μg/ml)
3 6 10
CLEC-2 Ab (μg/ml)
(iv)
WT
G6b hu/hu
ATP release (AUC)
10
8
6
4
2
0
1 3 10
CRP (μg/ml)
3 6 10
CLEC-2 Ab (μg/ml)
B (i)
collagen
WT
G6b hu/hu
G6b -/-
JON/A-PE
P-selectin-FITC
Annexin V-647
(ii)
Surface area coverage (%)
80
60
40
20
0
(iii)
Morphological score
6
4
2
0
WT
G6b hu/hu
G6b -/-
(iv)
Thrombus contraction score
(v)
Multilayer thrombus score
(vi)
Thrombus surface area coverage (%)
(vii)
JON/A-PE surface area coverage (%)
(viii)
P-selectin-FITC surface area coverage (%)
(ix)
Annexin V-647 surface area coverage (%)
C
Blood loss:body weight ratio (mg/g)
n.s.
WT
G6b hu/hu
G6b -/-

Figure 5

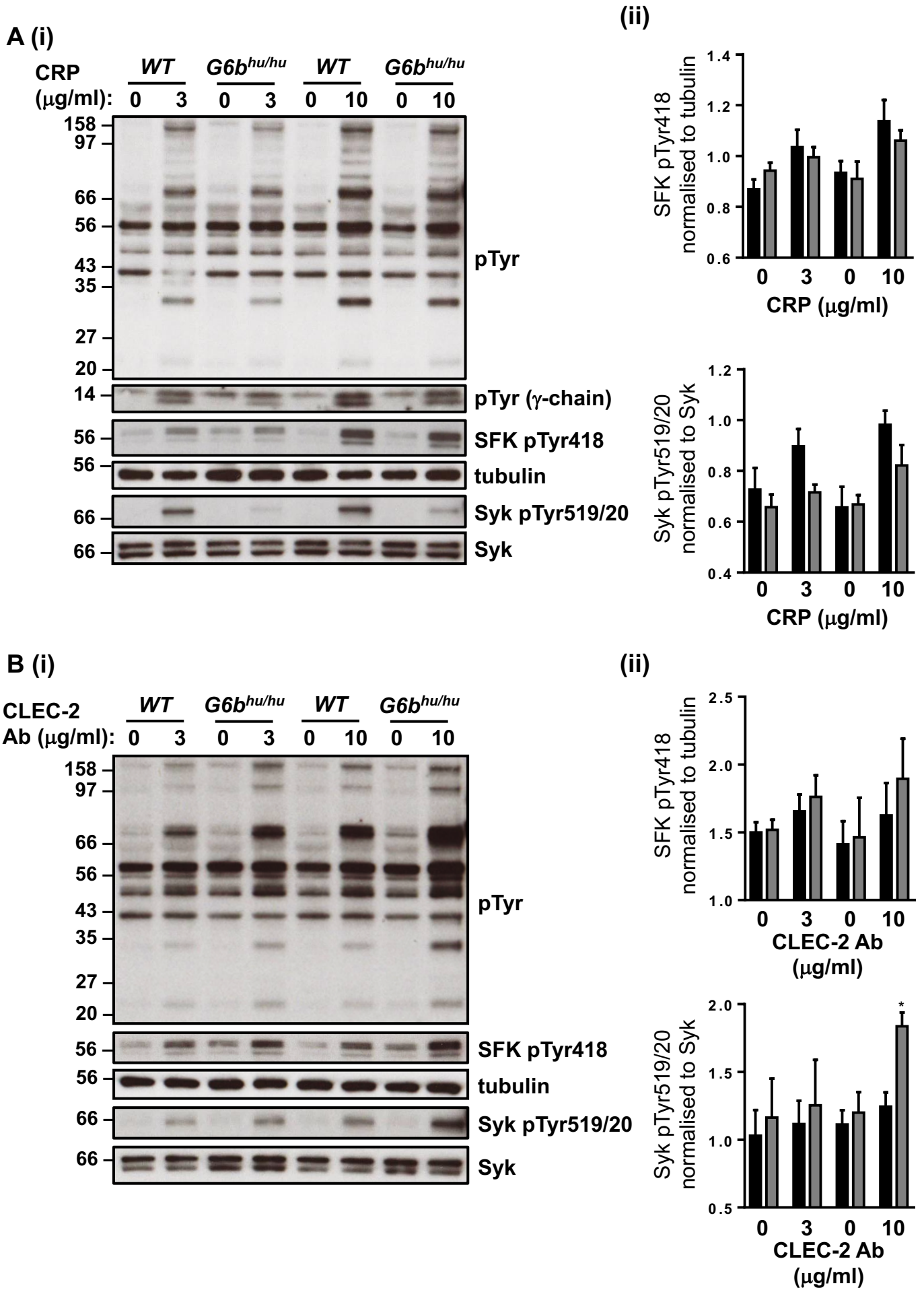
A (i)
CRP
(μg/ml):
WT
G6b hu/hu
WT
G6b hu/hu
0 3 0 3 0 10 0 10
158
97
66
56
43
35
27
20
14
56
56
66
66
pTyr
pTyr (γ-chain)
SFK pTyr418
tubulin
Syk pTyr519/20
Syk
(ii)
SFK pTyr418 normalised to tubulin
1.4
1.2
1.0
0.8
0.6
0 3 0 10
CRP (μg/ml)
Syk pTyr519/20 normalised to Syk
1.2
1.0
0.8
0.6
0.4
0 3 0 10
CRP (μg/ml)
B (i)
CLEC-2
Ab (μg/ml):
WT
G6b hu/hu
WT
G6b hu/hu
0 3 0 3 0 10 0 10
158
97
66
56
43
35
27
20
56
56
66
66
pTyr
SFK pTyr418
tubulin
Syk pTyr519/20
Syk
(ii)
SFK pTyr418 normalised to tubulin
2.5
2.0
1.5
1.0
0 3 0 10
CLEC-2 Ab (μg/ml)
Syk pTyr519/20 normalised to Syk
2.0
1.5
1.0
0.5
*
0 3 0 10
CLEC-2 Ab (μg/ml)

Figure 6

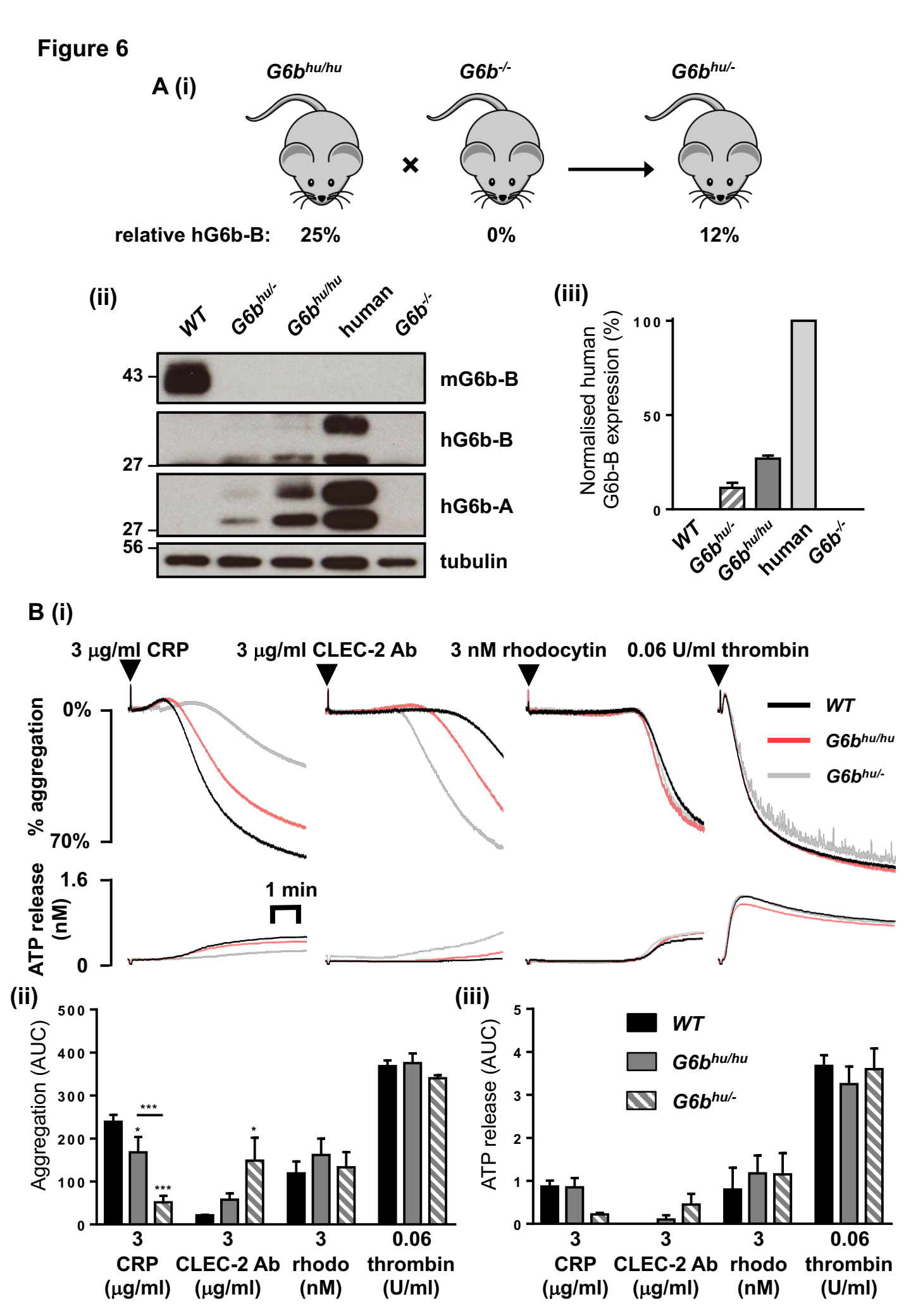
A (i)
G6b^hu/hu
G6b^-/-
G6b^hu/-
relative hG6b-B: 25% 0% 12%
(ii)
WT
G6b^hu/-
G6b^hu/hu
human
G6b^-/-
43
27
27
56
mG6b-B
hG6b-B
hG6b-A
tubulin
(iii)
Normalised human G6b-B expression (%)
100
50
0
WT
G6b^hu/-
G6b^hu/hu
human
G6b^-/-
B (i)
3 μg/ml CRP
3 μg/ml CLEC-2 Ab
3 nM rhodocytin
0.06 U/ml thrombin
% aggregation
0%
70%
ATP release (nM)
1.6
0
1 min
WT
G6b^hu/hu
G6b^hu/-
(ii)
Aggregation (AUC)
500
400
300
200
100
0
***
*
***
*
3 CRP (μg/ml)
3 CLEC-2 Ab (μg/ml)
3 rhodo (nM)
0.06 thrombin (U/ml)
(iii)
ATP release (AUC)
5
4
3
2
1
0
WT
G6b^hu/hu
G6b^hu/-
3 CRP (μg/ml)
3 CLEC-2 Ab (μg/ml)
3 rhodo (nM)
0.06 thrombin (U/ml)

Supplementary materials

Methods

Antibodies and reagents

FITC-conjugated P-selectin, GPVI, GPIbα and α2 and R-phycoerythrin (PE)-conjugated JON/A antibodies were from Emfret Analytics (Eibelstadt, Germany); PE-conjugated anti-αIIb antibody from BD Biosciences (Oxford, UK); phalloidin-488 from Thermo Fisher (Loughborough, UK); rat anti-mouse CLEC-2 antibody from Serotec (Oxford, UK) and Alexa488-conjugated goat anti-rat antibody from Life Technologies (Paisley, UK). G6b-B specific antibodies were raised as previously described.[33] For immunoblotting, anti-Shp1 and anti-Shp2 antibodies were from Santa Cruz Biotechnology (Dallas, TX, USA); anti-phosphotyrosine (p-Tyr) from Merck Millipore (Nottingham, UK); Src phosphotyrosine-418 (Src p-Tyr418) from Life Technologies (Loughborough, UK) and Syk phosphotyrosine-525/26 (Syk p-Tyr525/526) from Cell Signaling Technology (Hitchin, UK). All other reagents were from Sigma-Aldrich (Poole, UK), unless stated otherwise. Custom monoclonal mouse anti-human G6b extracellular domain, monoclonal rabbit anti-mouse G6b extracellular domain and polyclonal rabbit anti-human and –mouse G6b-B antibodies were generated by Biogenes (Berlin, Germany) as previously described (Mazharian et al, Sci Sign, 2012). Custom rabbit polyclonal antibodies for human G6b-A were raised against the intracellular tail of G6b-A (Biogenes, Berlin, Germany).

Genotype confirmation using Sanger sequencing

The *G6b* locus (NM_138272.2) was amplified with a single primer pair long range (LR) F & LR R1 with Bio-RadBioRad iProof HF master mix (Bio-Rad Laboratories, Hercules, CA), and sequenced with the same LR primers as well as primers designed to flank each exon. A description of the primers and Sanger sequencing conditions is shown in Supplementary Table 2.

DNA constructs

The cDNA encoding the human G6b-B protein was amplified by PCR from a human cDNA library. This PCR fragment was first cloned into the pCR®-Blunt vector (Invitrogen, Paisley, UK), and then subcloned into the pcDNA3 vector, for expression of untagged G6b-B in heterologous cell systems. The construct expressing the p.Gly157Arg mutant was generated by site directed mutagenesis (Genscript, Piscataway, NJ, USA).

Cell culture

DT40 chicken B cells were grown in RPMI supplemented with 10% fetal bovine serum, 1% chicken serum, 100 units (U)/ml penicillin, 100 μg/ml streptomycin, 50 μM β-mercaptoethanol, and 20 mM glutamine. 2 μg of *G6b-B WT*, *G6b-B Gly157Arg* or empty pcDNA3 vector were transfected by electroporation at 350 V and 500 microfarads into 2 x 10^7 cells DT40 cells, (resuspended in 400 μl serum free medium). Twenty hours after transfection, live cells were counted by trypan blue exclusion, and G6b-B expression levels were analyzed via flow cytometry and western blotting. Flow cytometry data presented as media fluorescence intensity.

G6b humanized mouse

To create the humanized G6b mouse, a targeting vector containing the human *G6b* genomic locus, a puromycin resistance cassette flanked by Flp-recombinase targeting sites and two homology arms was produced and inserted into the genome of C57BL/6NTac mouse embryonic stem cells by homologous recombination. Validated clones were injected into mouse blastocysts, before implanting into pseudo-pregnant female mice. Removal of the puromycin resistance cassette by a Flp recombinase expressing mouse subsequently allowed for *WT* and *KI* mice to be distinguished by PCR targeting the residual Flp-recombinase recognition site (Figure S1D, E). This *KI* strategy effectively knocked-out mouse *G6b* and allowed for physiologically normal promotor driven expression of human *G6b* in its place.

Mouse hematology

ACD anticoagulated whole blood was collected and blood cells counted using an ABX Pentra 60 hematological counter (Horiba Medical, Northampton, UK). Platelet count, platelet volume, white blood cell count and lymphocyte count data were normalized using a modified Box-Cox power transformation:

$$y' = \frac{(y^{\lambda} - 1)}{\lambda} + \lambda$$

When λ = 1: y' = y (No transformation)

When λ = 0: y' = ln(y) (natural log transformation)

Transformed data were verified to be normally distributed using Browne-Forsythe test for equal variance before being analyzed by one-way ANOVA with Dunnett's post-hoc test to compared each genotype to *WT*.

Flow cytometry

ACD anticoagulated whole blood were incubated with indicated FITC- and PE-conjugated antibodies before measuring using an Accuri C6 flow cytometer (BD Biosciences, Oxford, UK).

Platelet functional assays

Washed platelets (2×10^7/mL) were allowed to adhere and spread on fibrinogen-coated coverslips as previously described.[47] All slides were imaged using a Zeiss Axiovert 200M microscope and blinded images quantified using ImageJ. Stages of platelet spreading were categorized as unspread, formation of filopodia, formation of lamellipodia and fully spread (Figure S15). Platelet aggregation and ATP release was measured as previously described using washed platelets (2×10^8/mL) and a Chronolog Model 700 aggregometer.[48] ADP sensitive platelets were prepared as previously described.[49] For flow adhesion glass coverslips were coated as previously described,[50] and anti-coagulated whole blood (final concentrations: 40 μM PPACK, 5 U/ml heparin and 50 U/ml fragmin) flowed over for 3.5

minutes immediately following collection of blood. Images were captured with an EVOS microscope (Life Technologies, Carlbad, CA, USA) and blinded images analyzed using Fiji (Figure S11).

Supplemental Data: Clinical Case Descriptions

Family 1

Patient 1-III-1

Patient 1-III-1 was the male child of consanguineous parents (first cousins) of Arabic decent from the United Arab Emirates (UAE). The boy was born full term via normal spontaneous vaginal delivery (NSVD) following an uneventful pregnancy. The neonatal period was complicated by prolonged jaundice and dehydration. He was subsequently diagnosed with salt wasting due to congenital adrenal hyperplasia (CAH) due to 21-hydroxylase deficiency as a consequence of a homozygous intron 2 mutation (c.293-13C>G) in the *CYP21A2* gene). He was started on hydrocortisone and fludrocortisone supplementation with good clinical improvement. He was doing well until 5 months of age when he presented with prolonged epistaxis. A complete blood count (CBC) revealed anemia with a hemoglobin (HGB) of 5.0 g/dL and thrombocytopenia with $20x10^9$/L. The white blood cell count (WBC) was not available. The infant received packed red blood cells (PRBC) and platelet transfusions. His platelet count transiently improved to ~$100x10^9$/L. He remained thrombocytopenic with platelet counts ranging between 6-24 $x10^9$/L and required intermittent platelet transfusions (6 total). He also had a microcytic anemia with HGB ranging between 5-8 g/dL requiring occasional PRBC transfusions (3 total). The patient's bleeding symptoms were mild with occasional episodes of mild epistaxis and an episode of oozing from the bone marrow (BM) biopsy site requiring PRBC and platelet transfusion.

A BM aspirate and biopsy performed at another institution at 8½ months of age was interpreted as refractory cytopenia with myeloid dysplasia with no excess in blasts. Cytogenetics were reported to be normal. Concurrent blood counts showed a WBC count of $12.8x10^9$/L, HGB 9.3 g/dL with a mean corpuscular volume (MCV) of 72 fl and platelets of $16x10^9$/L. Hematopoietic stem cell transplantation (HSCT) was considered at the time but sibling donor evaluation was logistically difficult and HSCT was deferred.

Additional workup revealed a normal fetal HGB, negative viral studies (cytomegalovirus (CMV), Epstein-Barr virus (EBV)), no evidence of paroxysmal nocturnal hemoglobinuria (PNH) by flow cytometry and normal diepoxybutane (DEB) induced chromosomal breakage making an underlying Fanconi Anemia unlikely. His IgG was 592, IgA 63, and IgM 102. His lactate dehydrogenase (LDH) was elevated at 1091 (normal reference range 500-920). His peripheral blood (PB) smear showed mild leukocytosis, microcytic anemia with anisopoikilocytosis showing target cells, ovalocytes and thrombocytopenia with enlarged platelets. A repeat BM aspirate and biopsy at 13 months showed a hypercellular marrow for age with minimal granulocytic and erythroid dysplasia with a decreased myeloid-to-erythroid ratio (1:1) and moderate megakaryocytic dysplasia. Blasts were not increased. The biopsy revealed marked reticulin fibrosis. An iron stain was negative for ringed sideroblasts. Concurrent cytogenetic studies showed a normal male karyotype of 46, XY and negative fluorescence in situ hybridization (FISH) for del5q and monosomy 7. Overall the findings were thought to be consistent with a myeloproliferative or myelodysplastic process, although *JAK2* mutation analysis was negative.

Based on his persistent thrombocytopenia and anemia with ongoing transfusion needs he was referred for HSCT. A suitable matched sibling, unrelated donor or alternative donor was not available. Therefore, a haploidentical peripheral blood stem cell transplant (PBSCT) from the mother was done, using a submyeloablative conditioning regimen with Campath 1H, Fludarabine $30mg/m^2x4$ doses and total body irradiation (TBI) 600cGy

(HIMSUM, clinicaltrials.gov NCT00058825). Documentation of the cell dose and graft manipulation procedures were not available. Unfortunately, the patient failed to engraft with less than 10% BM cellularity comprised of all male karyotype cells on day 20 after his HSCT. He subsequently developed gram-negative bacterial sepsis and underwent a second haploidentical PBSCT from his mother ~50 days after his first PBSCT. Unfortunately, he developed progressive multiorgan failure, sever upper gastrointestinal bleeding due to a duodenal ulcer requiring several surgical interventions, renal and respiratory failure, and acute respiratory distress syndrome (ARDS), and succumbed from transplant related complications.

Patient 1-III-5

Patient 1-III-5, the 5-year old younger brother of 1-III-1, was born at full term via NSVD. He was cared for in the UAE during the first 10 months of his life. He was diagnosed with congenital adrenal hyperplasia (CAH) in the first week of life and received supplementation with hydrocortisone and fludrocortisone. He presented with bruising and petechiae on his upper chest on the first day of life. Given the family history of thrombocytopenia, a complete blood count (CBC) was obtained and showed a platelet count of $23x10^9$/L. He received a platelet transfusion with a post-transfusion count of $141x10^9$/L but quickly dropped again to 71 $x10^9$/L. His HGB and WBC were normal for age. A direct Coombs test was negative. A BM aspirate and biopsy at birth resulted in a non-diagnostic specimen. His initial workup included serology studies for TORCH infections (Toxoplasmosis, Other (syphilis, varicella-zoster, parvovirus B19), Rubella, Cytomegalovirus (CMV), and Herpes infections), which were negative. Mutation analysis for Wiskott-Aldrich syndrome was negative.

Given recurrent thrombocytopenia at 10 days of life he was treated with IVIG 1mg/kg IV x 2 days which improved his platelet count from $13x10^9$/L to $61x10^9$/L. Serial CBCs over the next several months documented platelet counts between 50 $x10^9$/L and $90x10^9$/L. By 6½

months of age he had recurrent severe thrombocytopenia to $16x10^9$/L and a new anemia with a HGB of 6.9 g/dL and received blood and platelet transfusions. A repeat BM showed a hypocellular, hemodilute aspirate with frequent lymphocytes. The biopsy revealed increased megakaryocytes and associated reticulin fibrosis similar to that seen in his older brother 1-III-1.

Beginning at 7-months of age, the patient became transfusion dependent for platelets, which he received every 10-days. He also required intermittent PRBC transfusions for a microcytic anemia. He never had leukopenia or neutropenia; his WBC was mildly elevated. He received a total of 3 IVIG treatment courses at day of life 10, and two- and four-months of age. He only showed a partial and transient improvement in his platelet count. His bleeding symptoms were mild to moderate with epistaxis, petechiae, frequent bruising and ecchymosis. He had one prolonged episode of epistaxis lasting for 12-hours, requiring transfusion support. The patient had normal growth and development and did not have hepatosplenomegaly on exam.

He transitioned care to our medical center at 10-months of age. A repeat BM aspirate and biopsy showed a cellular marrow with increased atypical megakaryocytes, occurring in clusters and associated marrow fibrosis. These findings confirmed the diagnoses of cMF and were consistent with those observed in his older brother. His genetic work up included negative mutation analysis for *MPL*, *JAK2* and *VPS45*.

The patient had the same identical human leukocyte antigen (HLA) type as his older brother (1-III-1). A repeat unrelated donor (URD) search did not reveal any acceptable HLA matched donors for HSCT consideration. In the meantime, the patient's aunt and uncle (also 1st cousins) had two additional children (1-III-8 and 1-III-9). 1-III-9 was found to be a 10/10 identical HLA match, but was also affected by CAH. She was considered as a related donor and underwent a work up to rule out cMF. Her CBC showed a mildly elevated WBC but no thrombocytopenia or anemia. Her marrow showed lymphoid aggregates with

mild fibrosis around the lymphoid aggregates. Her megakaryocytes were normal. Given the ongoing concern for an underlying inherited disorder we opted not to offer an upfront matched related donor (MRD) HSCT.

The patient remained transfusion dependent and treatment with a high dose steroid pulse (methylprednisone 30mg/kg x 3 days) followed by a slow taper was initiated. After 7-weeks he showed a partial response with platelet counts as high as $47x10^9$/L. A second steroid pulse with 1mg/kg methylprednisone was administered, to which his maximum platelet response was $89x10^9$/L. Unfortunately, the response was not sustained and his platelets decreased with the steroid taper, and ultimately reverted to $10x10^9$/L after he contracted primary varicella zoster infection.

Given that he remained transfusion-dependent, we re-considered the cousin (1-III-9) as the only MRD available. She underwent serial blood count and BM evaluations. Her blood counts remained normal and her BM on future studies was reassuring with normal megakaryocytes and minimal fibrosis in association with lymphocytes (see description below). None of those findings resembled those seen in the cousins and not diagnostic of cMF. The patient ultimately underwent a MRD HSCT from his cousin at 2-years of age. The patient was conditioned with a fully myeloablative conditioning regimen with busulfan and cyclophosphamide and received cyclosporine (CSA) and a short course of methotrexate (MTX) for graft-versus-host disease (GVHD) prophylaxis. Bone marrow was used as stem cell source with a cell dose of $4.32x10^8$ total cells/kg. His transplant course was uncomplicated without major infections, organ toxicity or GVHD. He engrafted myeloid cells on day +34 and became RBC transfusion independent on day +39. He had delayed platelet engraftment, becoming transfusion independent on day +60 and reached over $100x10^9$/L on day + 178. Blood counts at 21-months post-transplant were entirely normal with a WBC of 10.61 $x10^9$/L, HGB 13.7 g/dL, and platelets 343 $x10^9$/L. His MCV was normal at 80.5 fl (previously microcytic).

His BM aspirate and biopsy 4 and 8 months after HSCT showed a mildly hypocellular marrow with maturing trilineage hematopoiesis and a mildly increased myeloid-to-erythroid ratio. Megakaryocytes were present in normal numbers and morphology. Reticulin was minimally increased but markedly decreased from his pre-HSCT BM studies. All concurrent cytogenetic studies showed a normal female karyotype and negative FISH for monosomies 5 and 7, trisomy 8 and partial deletions of long arms of chromosomes 5, 7 and 20. Whole blood chimerism showed slight decrease in donor chimerism (93% donor, 7% recipient) but his blood counts remained normal.

Patient 1-III-6

During our evaluation of 1-III-5, the mother of 1-III-1 was pregnant with another male fetus. Amniocentesis confirmed that the fetus also had an intron 2G mutation in the *CYP21A2* gene and would be affected by CAH. HLA typing on the amniotic material showed the same homozygous HLA type found in his two older brothers (1-III-1 and 1-III-5). The baby was born full term and managed for his CAH. Given the family history of cMF, blood counts were followed closely. His platelet count at birth was $50x10^9$/L, but recovered to $132x10^9$/L and $270x10^9$/L at 2 and 4 weeks of life, respectively. A repeat evaluation at 5 months of age, however, showed leukocytosis, microcytic anemia and thrombocytopenia with a WBC of $13.79x10^9$/L, HGB 8.7 g/dL and platelets of 19 $x10^9$/L, raising concern that the infant was affected by cMF as well. A BM showed findings identical to his two affected brothers, including increased reticulin fibrosis and atypical megakaryocytes. Concurrent cytogenetics studies were normal. The patient, who was HLA identical to his brothers (1-III-1 and 1-III-5) and cousin (1-III-9) was carefully monitored while his older brother underwent a MRD HSCT from their cousin, 1-III-9. Between age 5 and 16 months of age his platelet count ranged from 15 to 25 $x10^9$/L. His WBC and HGB ranged from 6.2 to $17.17x10^9$/L and 7.8 to 9.7g/dL respectively. During this period of observation, he received three platelet transfusions and showed mild bleeding symptoms, including several hematomas and

episodes of epistaxis. He returned to the UAE, where, at 17-months of age, he had significant gum bleeding and epistaxis and received platelet transfusions, but did not show an improvement in his platelet count. He received a dose of IVIG, which transiently improved his platelets to $100x10^9$/L. A repeat BM at 14-months of age showed normocellular marrow for age (95% cellularity), increased atypical megakaryocytes often occurring in clusters, and worsening reticulin fibrosis (grade 3). His genetic work up included negative mutation analysis for *MPL, JAK2* and *VPS45*.

Given the successful HSCT of his older sibling from their fully matched related donor, and the lack of another related, unrelated or alternative donor source, we opted to perform the same HSCT for this patient. Prior to proceeding we confirmed that the donor remained unaffected with normal blood counts and a normal BM aspirate and biopsy. 1-III-6 underwent a fully MRD HSCT with myeloablative conditioning regimen comprised of busulfan and cyclophosphamide. GVHD prophylaxis consisted of cyclosporine A (CSA) and a short course of methotrexate (MTX). His transplant course was largely uncomplicated. He had delayed myeloid engraftment at day +45 and delayed platelet and red cell engraftment requiring intermittent platelet transfusion. A BM study on day +95 showed a mildly hypocellular marrow for age with normal myeloid-to-erythroid ratio and normal maturation. Megakaryocytes were mildly decreased but morphologically normal. Reticulin stain did not show evidence of reticulin fibrosis. Serial BM chimerism studies showed over 97% donor chimerism in all lineages (T-cells, B-cells and myeloid fraction). His laboratory studies showed evidence of hemolysis and it was felt his anemia and thrombocytopenia might be due to mild transplant-associated thrombotic microangiopathy (TA-TAM) due to CSA, and he was switched with Tacrolimus for GVHD prophylaxis. He received several doses of darbopoietin due to low erythropoietin levels.

His anemia and thrombocytopenia slowly improved beginning day +120 after his HSCT. His HGB level eventually normalized on day +136. Other than mild chronic oral GVHD at day

+150, for which he was treated with topical steroids and topical tacrolimus, he experienced no significant organ toxicities or infections.

Due to persistent thrombocytopenia a repeat marrow was performed 1 year post-HSCT and showed a mildly hypocellular marrow for age with maturing trilineage hematopoiesis and no evidence of reticulin fibrosis. Megakaryocytes were mildly decreased, occasional occurred in small clusters but morphologically normal appearing. His BM chimerism studies remained 100% donor.

Patient 1-III-9

1-III-9 is the cousin of proband 1-III-1 and his brothers 1-III-5 and 1-III-6. She is the product of a consanguineous relationship (first cousins) of Arabic decent from the United Arab Emirates. The parents of 1-III-1 and 1-III-9 are siblings to each other (Figure 1A).

Individual 1-III-9 was also diagnosed with CAH shortly after birth. She underwent surgical correction with vaginoplasty. HLA typing in search for a potential related donor for 1-III-5 showed an identical homozygous HLA type to the proband 1-III-1, 1-III-5 and 1-III-6. She was considered as a potential marrow donor for 1-III-5. Given the concern for an underlying inherited cause of the families' cMF she underwent careful diagnostic evaluation, which included serial CBCs that were all normal. A BM study at 14-months of age showed a normocellular marrow for age with numerous lymphoid aggregates that contained germinal centers. The myeloid-to-erythroid ratio was increased. Myeloid and erythroid elements showed normal maturation and no dysplasia. Megakaryocytes were normal in number and morphology. Reticulin stain showed a slight increase in reticulin in association with the lymphoid aggregates. Concurrent cytogenetic and FISH studies for monosomies 5 and 7 and trisomy 8 were negative. Lymphoid aggregates at this age can be seen in autoimmunity, but a detailed family history and screening laboratory studies for an autoimmune disorder were negative. Given the unknown significance of the lymphoid aggregates in the marrow, her donor status for her male cousin (1-III-5) was placed on hold.

A repeat BM at 16 months showed resolution of the lymphoid aggregates and no evidence of a cMF.

Her cousin 1-III-5 was treated with high dose steroids (see above) but did not show a sustained response and remained transfusion dependent. We therefore performed a reevaluation of 1-III-9. Blood counts remained entirely normal with WBC $8.39x10^9$/L, HGB 11.9 g/dL, platelet count $468x10^9$/L. A repeat BM at 2 years and 6 months showed a normocellular marrow for age with maturing trilineage hematopoiesis with relative erythroid and mild megakaryocytic hyperplasia.

Given the lack of features diagnostic of cMF and the ongoing transfusion needs of her cousin 1-III-5, we discussed treatment options with both families. After carefully consideration, informed consent regarding the theoretical risk for an underlying genetic diagnosis for which 1-III-9 could be a non- or minimally- expressing carrier, 1-III-9 was used as a marrow donor for 1-III-5. The transplant was successful with prompt myeloid engraftment and delayed platelet engraftment likely due to remodeling of hematopoietic niche due to reticulin fibrosis. Ultimately 1-III-5 achieved robust trilineage engraftment with normal blood counts and a normal marrow.

A follow up marrow was performed at 4-years of age to assess if she could serve as a donor for the other cousin, 1-III-6, who was also platelet transfusion dependent. The BM showed a mildly hypocellular marrow for age with maturing trilineage hematopoiesis and normal myeloid and erythroid maturation. Megakaryocytes were present in normal numbers and morphologically unremarkable. Reticulin fibrosis was not present. No lymphoid aggregates were noted. The blood counts remained normal.

Family 2

Patient 2-II-6

The proband (2-IV-6) is a child of a consanguineous family of Arabic decent; the parents are first cousins from Saudi Arabia (Figure 1). The patient was a male born at 36 weeks via caesarian section due to premature rupture of membranes and fetal distress. He required a brief period of non-invasive ventilation with a neonatal intensive care unit (NICU) stay of 1-month. During his first month of life, serial CBCs were performed, which showed mild thrombocytopenia with a platelet count of $112x10^9$/L with a normal HGB and WBC count. His platelet count improved to $161x10^9$/L by the time of discharge. He had a follow up CBC at 3 months of age, which showed a normal platelet count of $220x10^9$/L, HGB 10g/dL, and MCV of 97fl. WBC was reported as "normal". The patient was doing well until 6-months of age when a routine CBC showed severe thrombocytopenia (platelet count $10x10^9$/L) and microcytic anemia (HGB 5.4g/dL, MCV 65fl). He received RBC and platelets transfusion and was treated for a presumed immune mediated cytopenia and with IVIG and steroids. He showed some improvement in his blood counts with a maximum platelet count of $127x10^9$/L. Unfortunately, the improvement in his platelet count was never sustained and his platelet count dropped as soon as steroids were tapered. He received a total of 4 courses of steroids and several doses of IVIG. The patient required 6-8 RBC and approximately 10 platelet transfusions. His microcytic anemia was treated with iron supplementation, but did not lead to improvement in his anemia.

From a clinical perspective, he showed objective signs of bleeding including mucosal bleeding (lower gastrointestinal and oral mucosa), easy bruising and oozing from a bone marrow procedure site, requiring a transfusion. He had mild decrease in energy due to anemia. Three BM studies were performed at 12-, 14- and 24-months and overall showed a normocellular marrow with trilineage hematopoiesis and normal numbers of megakaryocytes. Reticulin stain at 24-months was negative.

A follow up marrow at 3 years of age showed a hypercellular marrow for age with maturing trilineage hematopoiesis and increased lymphocytes, including young forms and hematogones and moderate myelofibrosis (reticulin fibrosis grade 1-2+).

His work-up included normal blood chemistries, liver function tests, iron studies, ferritin 45, iron saturation 45% and elevated hepcidin of 437.5 ng/ml. Vitamin B_{12}, Vitamin D, and folate were normal. Platelet autoantibodies were detected against GP IIb/IIIa and Ib/IX. An autoimmune work up (ANA, auto-antibody screen) and autoimmune lymphoproliferative syndrome (ALPS) panel was negative. Lymphocyte subsets and immunoglobulins were normal, except IgM was decreased at 30 mg/dL. A gene sequencing panel for inherited BM failure syndromes, globin disorders and myeloproliferative neoplasms (*JAK2, MPL, CALR*) and *VPS45* was negative. Platelet function and aggregation studies could not be performed due to low platelet count.

Due to concern for a congenital disorder and the potential need for HSCT, HLA typing was performed revealing a homozygous HLA type, although different from that present in Families 1 and 3.

Patient 2-II-5

Patient 2-IV-5 is the older brother of 2-IV-6 who was noted to have macrothrombocytopenia on a CBC following his brother's diagnosis. He has a stable platelet count, ranging from 45 to $107x10^9$/L. His blood counts and smear showed mild leukopenia, no neutropenia, aniso- and poikilocytosis with a HGB of 8.8g/dL.

All of the siblings of the other siblings are reported to have iron deficiency anemia with a HGB of <10 g/dL. All of the father's sisters are reported to have iron deficiency anemia and are reported to be on iron supplementation. Platelet counts in those relatives are thought to be normal. The family history was also significant for diabetes and hypertension in the grandparents, liver cancer in the father's aunt and gastric cancer in the grandmother. There is no history of bleeding disorders or thrombocytopenia.

Family 3

Patient 3-II-4

The proband (3-IV-4) was referred to our medical center at 18-months of age for work up of cMF. She was born at full-term and is the 4th living child of a consanguineous family (parents are first cousins) from the UAE (Figure 1). At birth, the patient had ambiguous genitalia and was diagnosed with CAH due to 21-hydroxylase deficiency. She has been managed with hydrocortisone and fludrocortisone. She was doing well until 15 months of age when she was found to be pale. Her blood counts showed leukocytosis (WBC 19.2 cells x10^9/L), microcytic anemia (HGB 5.1g/dL, MCV 71.3, reticulocytes 1.5%) and thrombocytopenia 81 x10^9/L. She did not have any hepatosplenomegaly, lymphadenopathy or dysmorphic features. The peripheral blood smear demonstrated anemia with marked anisopoikilocytosis (target cells, schistiocytes) and occasional nucleated red blood cells. Leukocytosis with left myeloid cells and immature forms and thrombocytopenia with variable sized platelets including larger forms was noted. Platelet granulation was normal.

A BM aspirate and biopsy showed a mildly hypercellular marrow for age (90% cellularity) with a relative myeloid hyperplasia. Myeloid and erythroid elements matured normally. Megakaryocytes were increased, showed variable morphologic abnormalities including small hypolobated forms, and occurred in clusters. Blasts were not increased. Scattered small lymphocytes appeared normal. Mildly increased eosinophils were noted. A reticulin stain showed mild to moderately increased fibrosis (grade 1-2 out of 3). Immunohistochemistry (IHC) for CD61 showed increased megakaryocytes, focally clustering. The BM aspirate was hypocellular and aspicular and likely not representative, due to marrow fibrosis.

Her work-up included a normal chest x-ray with no bony abnormalities. She underwent an abdominal ultrasound to evaluate possible hepatosplenomegaly and was found to have asplenia. Laboratory testing was negative for nutritional deficiencies (iron, B_{12}, folate).

1,25-dihydroxy Vitamin D was mildly elevated at 89.2. Chemistry studies including liver function tests, electrolytes, and creatinine were normal. Her LDH was elevated at 446 with a negative direct Coombs test. Her immunology workup showed normal immunoglobulin levels (IgG, IgA, IgM) and a largely unremarkable lymphocyte subsets with a slight increase in CD19+ B-cells and mild decrease in CD3+ T-cells). Her molecular work up included sequencing analysis for *JAK2, MPL, CALR* and *VPS45*, all of which were negative.

The patient has 3 full biological siblings ages 3-, 7- and 8- years old, all of which are reported to be healthy but could not be fully assessed given that they were in their home country at the time of evaluation at our center. There is no family history of thrombocytopenia or anemia. A now 27-year-old aunt on the maternal side was diagnosed with acute leukemia at age 8 years and has been in remission since.

Family 4

Patient 4-II-2

Patient 4-II-2 is the second male child of consanguineous parents (first cousins) of Arabic decent from Algeria. The boy was born full term via NSVD following an uneventful pregnancy. He was seen at 18 months when a CBC revealed a severe microcytic anemia (5.1 g/dL) with low ferritin level (4ng/mL) and thrombocytopenia ($96x10^9$/L). His anemia improved to 11.5 g/dL with hemoglobin F level (4%). He has a normal WBC of $6.44x10^9$/L but a persistent severe thrombocytopenia with a platelet count between $10\text{-}30x10^9$/L. The patient continued to be followed with supportive care and is now 25-years old at last follow up. He continues to have persistent thrombocytopenia with platelet counts under $10x10^9$/L. He received IVIG and steroid therapy with no response, but has transient improvements in his platelet count after a platelet transfusion. The peripheral blood smear showed hypogranulated and gray platelets with a normal mean platelet volume. The red cells showed microcytosis, anisiopoikylocytosis with leptocytes, spherocytes, dacrocytes and occasional Howell-Jolly bodies. A partial deficiency in alpha granules in a subset of the

platelets was confirmed by electronic microscopy. The levels of platelet glycoproteins GPIb, GPIIbIIIa, GPIV studied by flow cytometry were normal. The patient did not show any clinical bleeding. He did have a cerebral cavernous malformation (cavernoma) but no other syndromic abnormalities. Two BM biopsies performed at 13 and 15 years of age were similar and showed erythroid dysplasia without blasts excess, dysmegakaryopoiesis with numerous hypobulated and small megakaryocytes. Reticulin staining showed marked reticulin fibrosis (stage II). Additional investigations revealed normal BM cytogenetics and a normal diepoxybutane induced chromosomal breakage studies. Molecular sequencing analysis was negative for mutations in *WAS, GATA1, FOG, c-MPL, RUNX1, NBLEA2, TERC, TERT, TINF2* and *DKC1*. The patient's maternal grandfather deceased at the age of 65 of a myelodysplastic syndrome with blasts excess.

Patient 4-II-3

The proband's (4-II-2) sister presented with thrombocytopenia in her first year of life but was not diagnosed until 11 years of age. Her peripheral blood cell count showed leukocytosis (WBC 17 $X10^9$/L), a normal hemoglobin level (12.5 g/dL) with a normal hemoglobin F level, and mild thrombocytopenia with a platelet count of $97x10^9$/L. The patient continued to be followed and was 23-years old at the last follow up. She had persistent mild to moderate thrombocytopenia with platelet counts between 80-$140X10^9$/L. She has not had any bleeding symptoms despite three surgical procedures. Her PB smear showed anisopoikylocytosis with target cells, rare schistocytes, leptocytes, dacryocytes and occasional Howell-Jolly bodies. The majority of her platelets showed a normal platelet volume (91%) with a small subset showing an increased platelet volume (9%). Some platelets showed decreased granulation (gray platelets, 8%). Platelet function assays were normal. A BM biopsy revealed a hypercellular marrow with dysmegakaryopoiesis and numerous micromegakaryocytes, moderate erythroid dysplasia without blast excess and normal granulopoiesis. A marked reticulin fibrosis stage II was detected.

Table S1

Genotype	Observed frequency	Predicted frequency
WT (+/+)	38 (26%)	37 (25%)
Het (+/hu)	72 (50%)	72 (50%)
Hom (hu/hu)	35 (24%)	36 (25%)

Data collected from 10 breeding pairs, average litter size 6 pups.

Table S2

Amplicon Primers (5’-3’)	
MPIG6B LR_F	ATCACAATCCCCTACAAAACAGG
MPIG6B LR_R1	GGAGAGGGATTATGGGGAGC
Sequencing Primers (5’-3’)	
MPIG6B 1F	GTTCTCCCCACGCCTAACTT
MPIG6B 1R	ATCTTCCCACACACAACCCA
MPIG6B 2F	GAAAGAGGAGACGGGATGGA
MPIG6B 2R	CCTCCTCCGGGTATGTGTC
MPIG6B 3F	CTGGCTGTCCCTCGTCAAA
MPIG6B 3R	TTTTGCGAAGGTTCTGGTCC
MPIG6B 4_5F	TGTCGGTGGGGTAGAGTCTA
MPIG6B 4_5R	GGAGAGGGATTATGGGGAGC

Figure S1

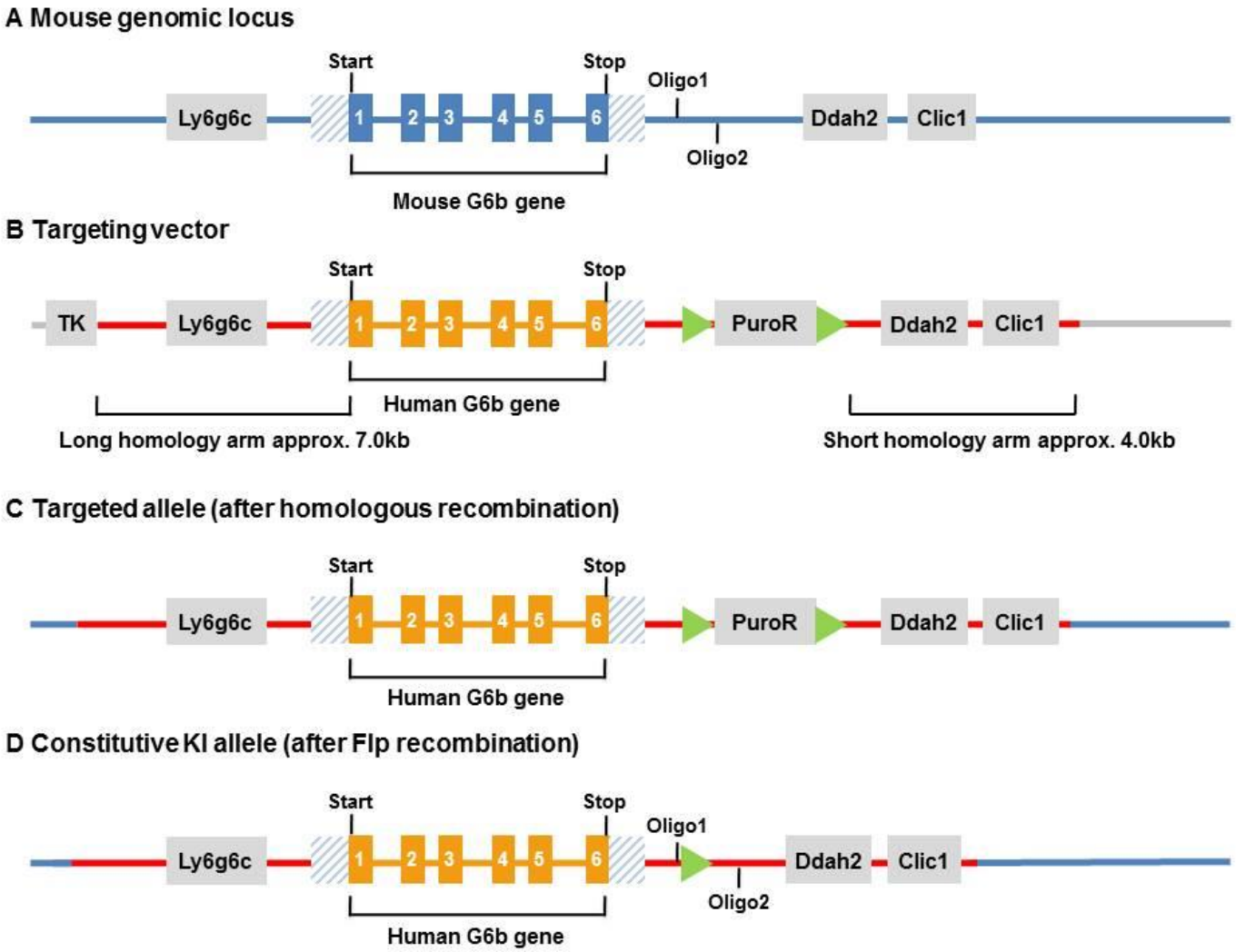
A Mouse genomic locus
Start
Stop
Oligo1
Ly6g6c
1
2
3
4
5
6
Ddah2
Clic1
Oligo2
Mouse G6b gene
B Targeting vector
Start
Stop
TK
Ly6g6c
PuroR
Ddah2
Clic1
Human G6b gene
Long homology arm approx. 7.0kb
Short homology arm approx. 4.0kb
C Targeted allele (after homologous recombination)
Start
Stop
Ly6g6c
PuroR
Ddah2
Clic1
Human G6b gene
D Constitutive KI allele (after Flp recombination)
Start
Stop
Oligo1
Ly6g6c
Ddah2
Clic1
Oligo2
Human G6b gene
G6b exon
G6b untranslated region
Human G6b exon
Neighbouring gene
Mouse genomic region
Vector knock-in region
Vector region
Human genomic region
Flippase recognition target
Oligo PCR primer target
Start Start codon
Stop Stop codon

Figure S1

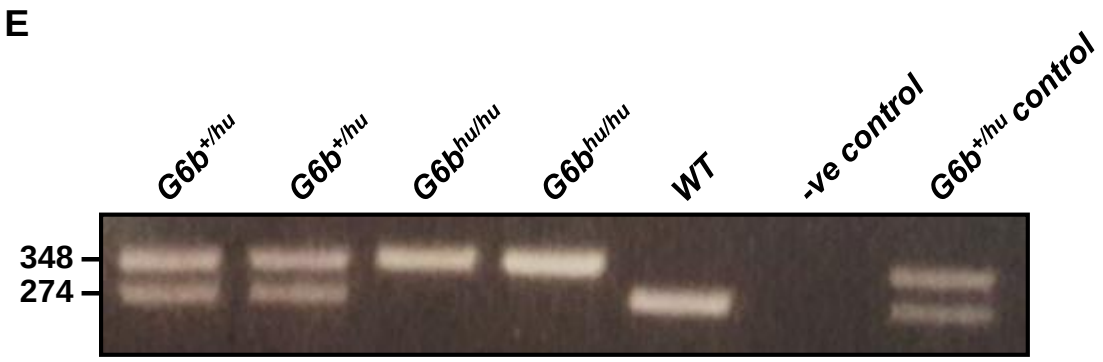

Figure S1. A constitutive knock-in strategy was used by Taconic to insert the human *G6b* allele into (A) the genomic locus of mouse *G6b*. (B) A targeting vector containing human *G6b* and a puromycin resistance cassette flanked by Flp recombinase sites was produced. (C) The two homology arms of the targeting vector flanking the human gene provided sites for homologous recombination to insert human *G6b* into the C57BL/6NTac embryonic stem cell genome. (D) The puromycin resistance was removed by crossing mice expressing the human *G6b* allele with a Flpe recombinase expressing mouse producing the final constitutive knock-in allele. (E) Oligos 1 and 2 were used to distinguish *WT* and *KI* mice by PCR.

Figure S2

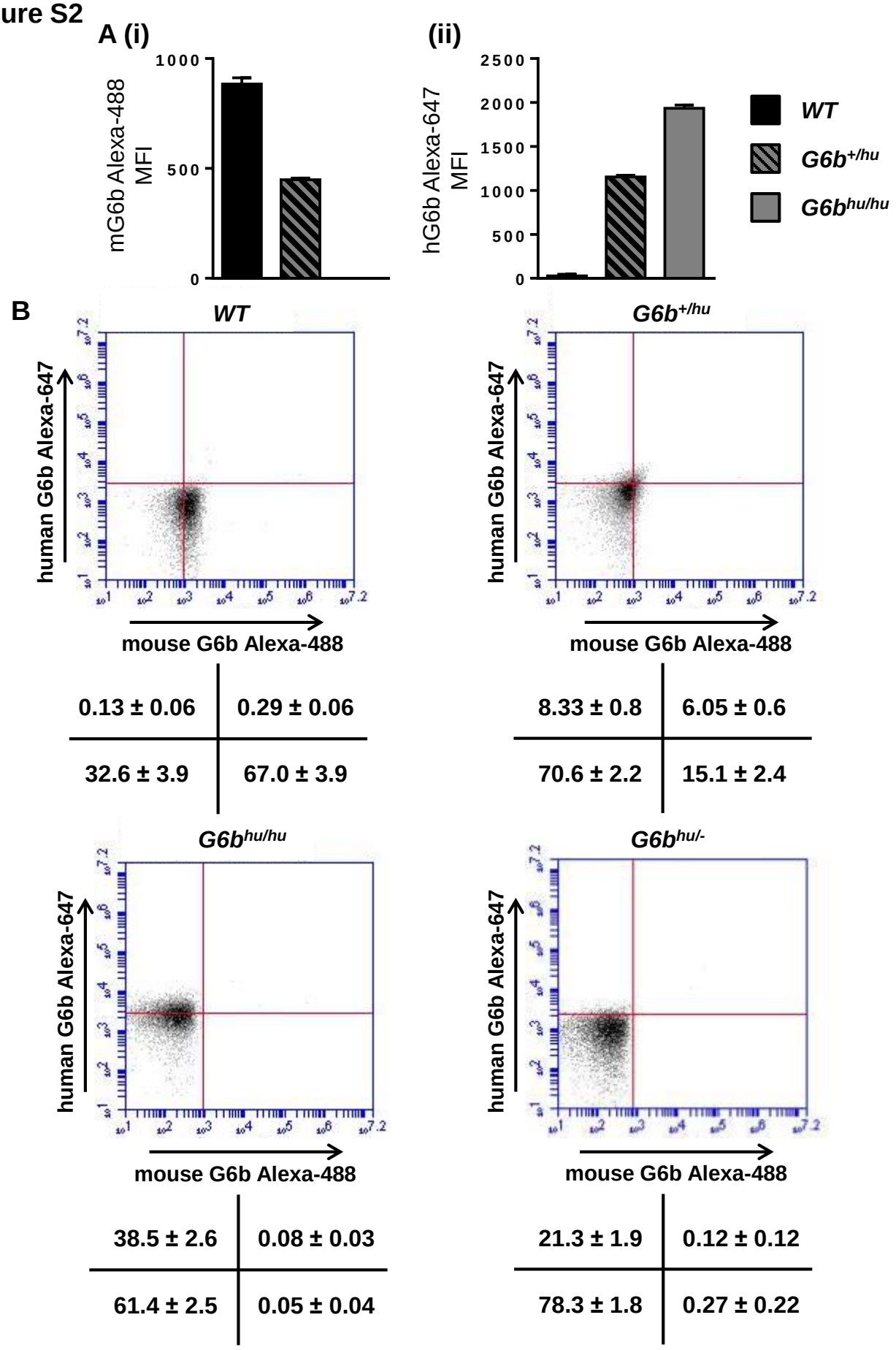

Figure S2. (A) mouse (m)G6b and human (h)G6b median fluorescence intensity (MFI), mean ± SEM, n=6. (B) Representative density plots and mean ± SD of percentage of events in each quadrant (n=6).2

Figure S3

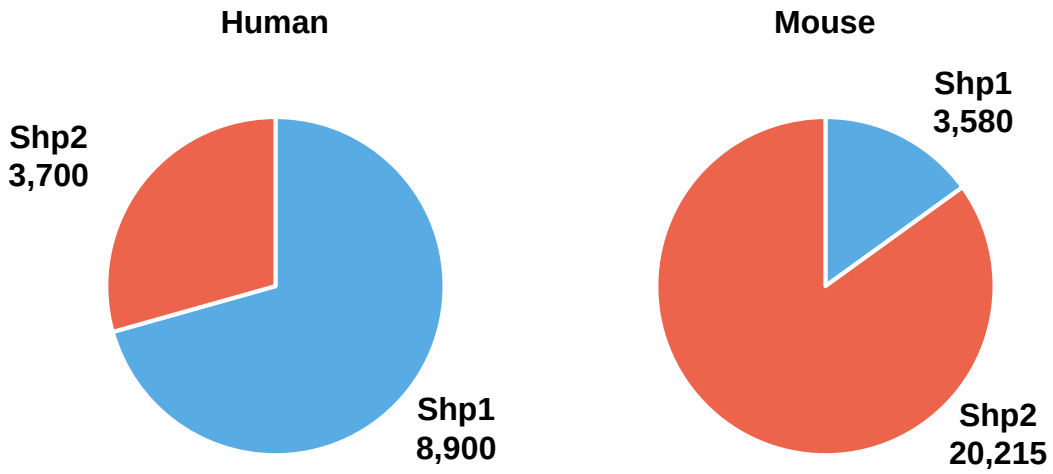

Figure S3. Relative proportions of Shp1 (blue) and Shp2 (red) expression in human and mouse platelets. Numbers indicate copy number per platelet as measured by quantitative proteomic studies (Burkhart et al, 2012 and Zeiler et al, 2014)

Figure S4

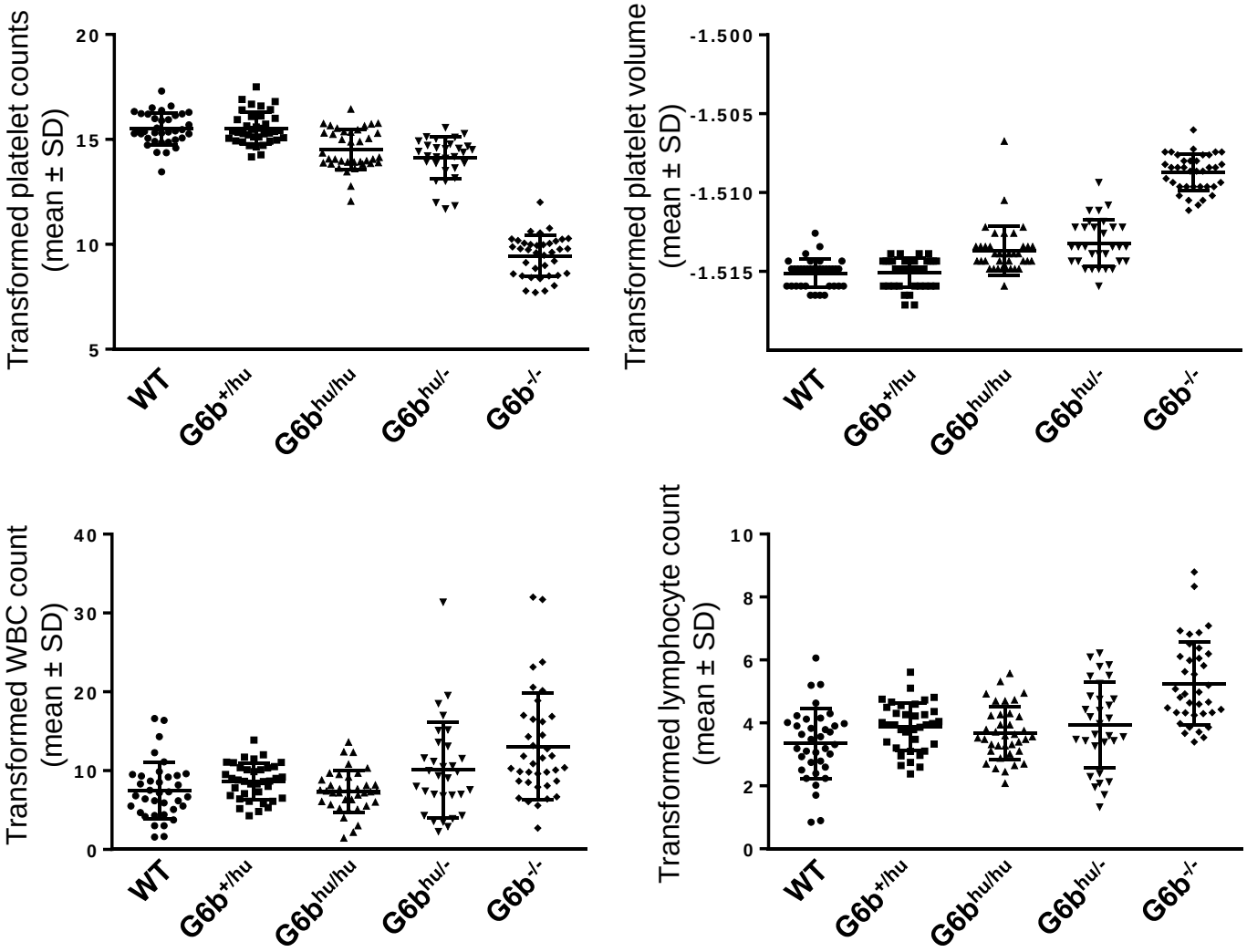

Figure S4. Distribution of transformed blood cell counts used for statistical analysis. Platelet count, platelet volume, white blood cell (WBC) count and lymphocyte count data were transformed using a modified Box-Cox power transformation and normality of distribution verified using Browne-Forsythe test for equal variance. Transformed data were used for analysis by one-way ANOVA and Dunnett's post-hoc test to compare all genotypes to *WT*.

Figure S5

A

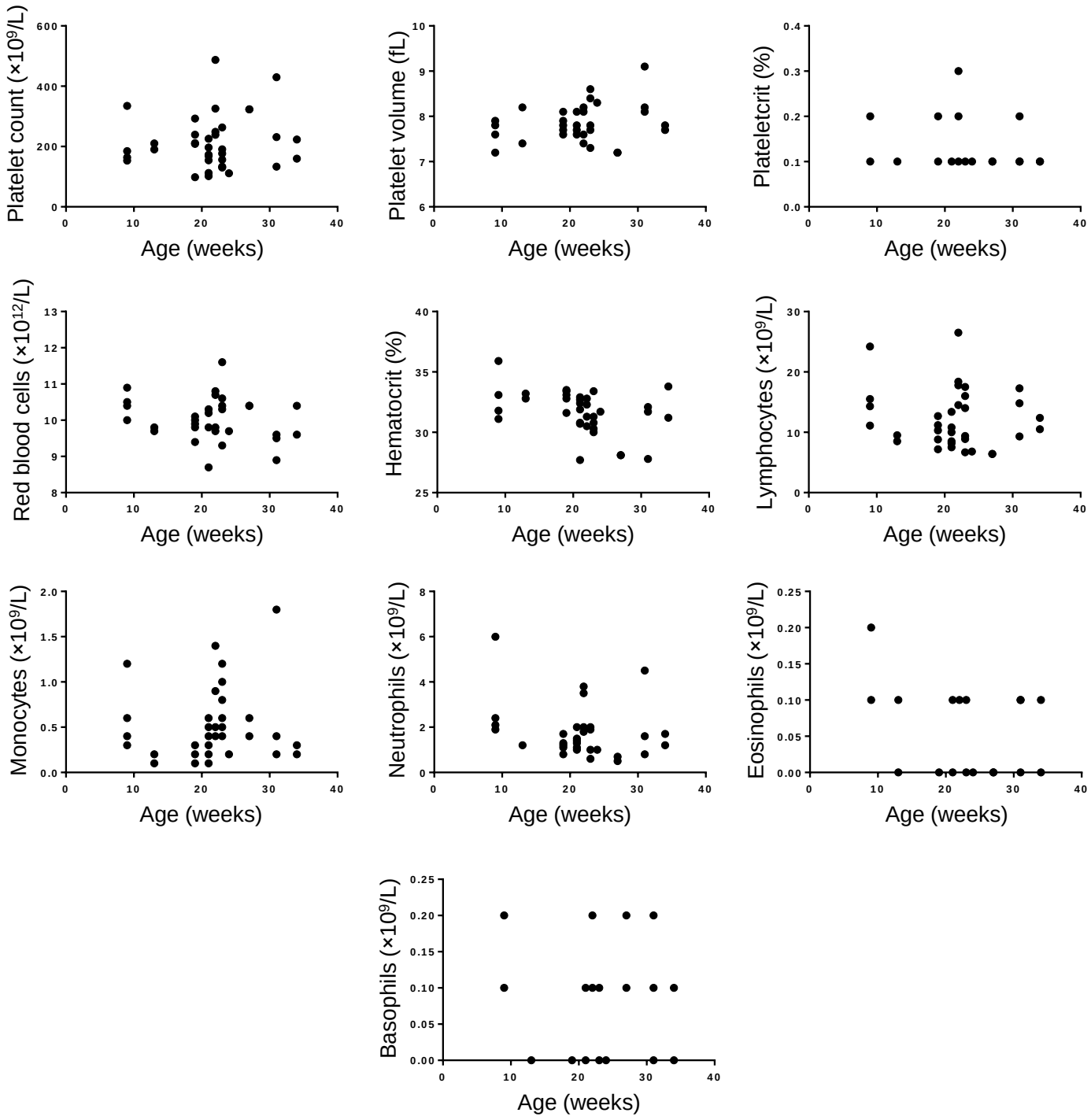

B

	Platelet count	Platelet volume	Plateletcrit	Red blood cells	Hematocrit	Lymphocytes	Monocytes	Neutrophils	Eosinophils	Basophils
R^2	0.01	0.06	0.00	0.04	0.14	0.02	0.01	0.05	0.07	0.00
P-value	0.50	0.15	0.84	0.21	0.02	0.40	0.58	0.17	0.11	0.08

Figure S5. Blood cell counts variation is independent of age in *G6b KO* mice. (A) Blood cell counts were plotted against age for *G6b KO* mice (n=37). (B) Regression analysis indicates that there is no correlation between age and hematological parameters.

Figure S6

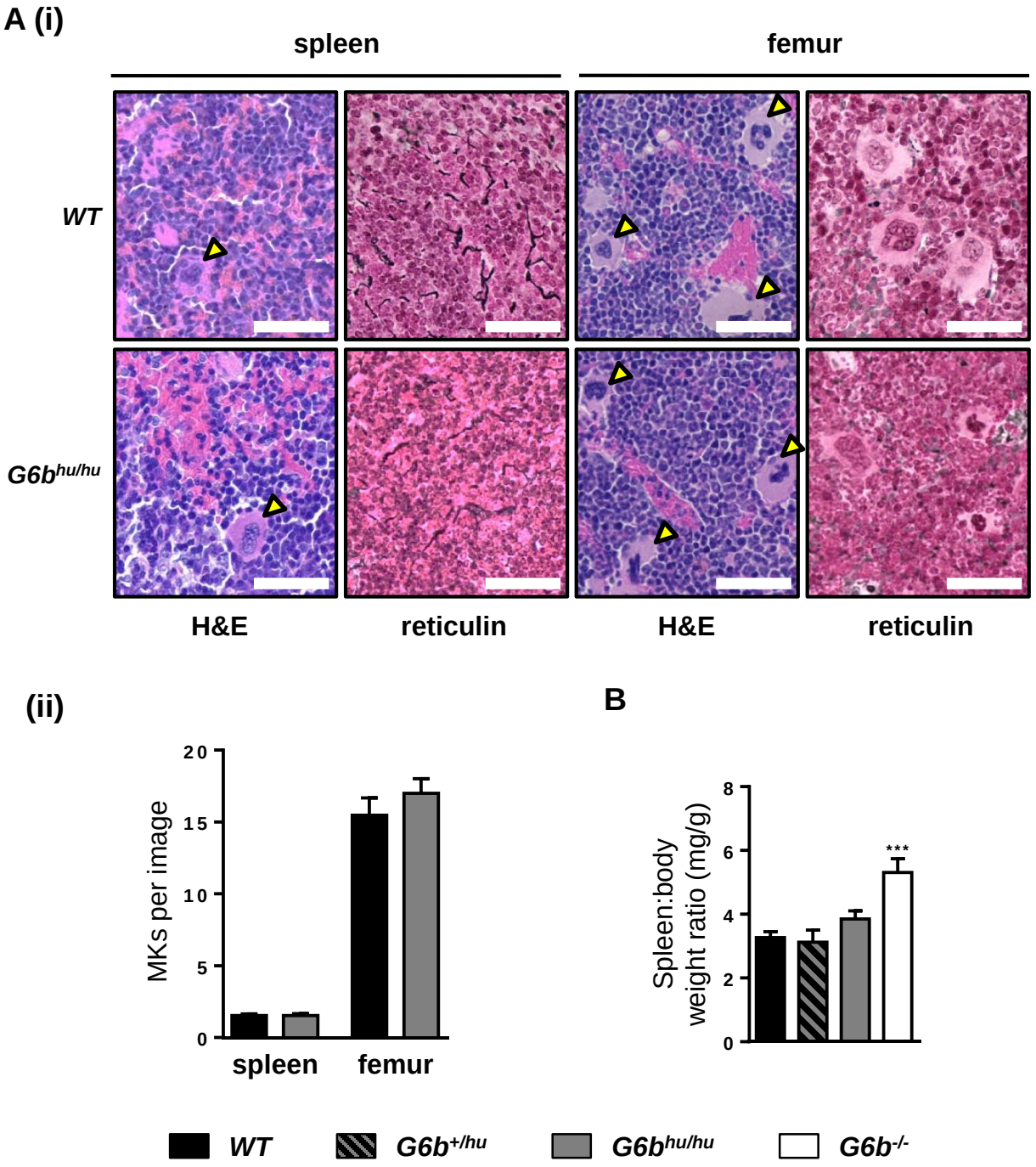

Figure S6. (A) Representative images of H&E and reticulin stained *WT* and *G6b*$^{hu/hu}$ mouse spleens and femurs and quantification of megakaryocytes (MKs) in spleen and femur sections (n=6). (B) Spleen to body weight ratio of indicated genotypes (n=3-30). All data represented as mean ± SEM. Scale bar: 50 μm.

Figure S7

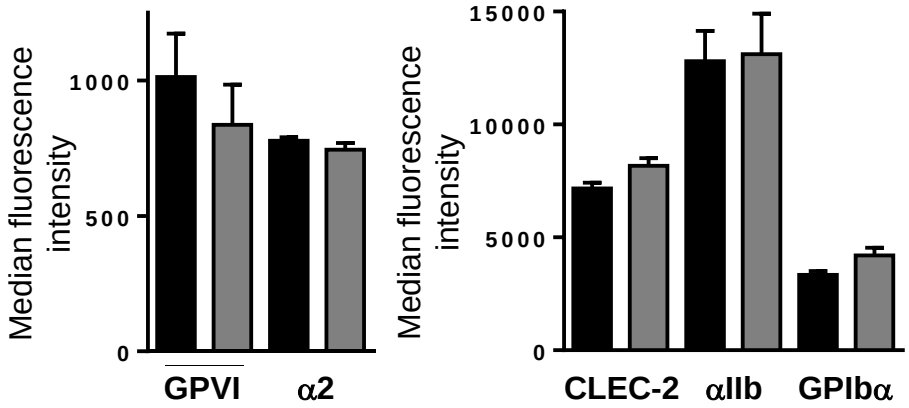

Figure S7. Surface expression of the major platelet receptors in *WT* and *G6b*$^{hu/hu}$ mice. All data represented as mean ± SEM.

Figure S8

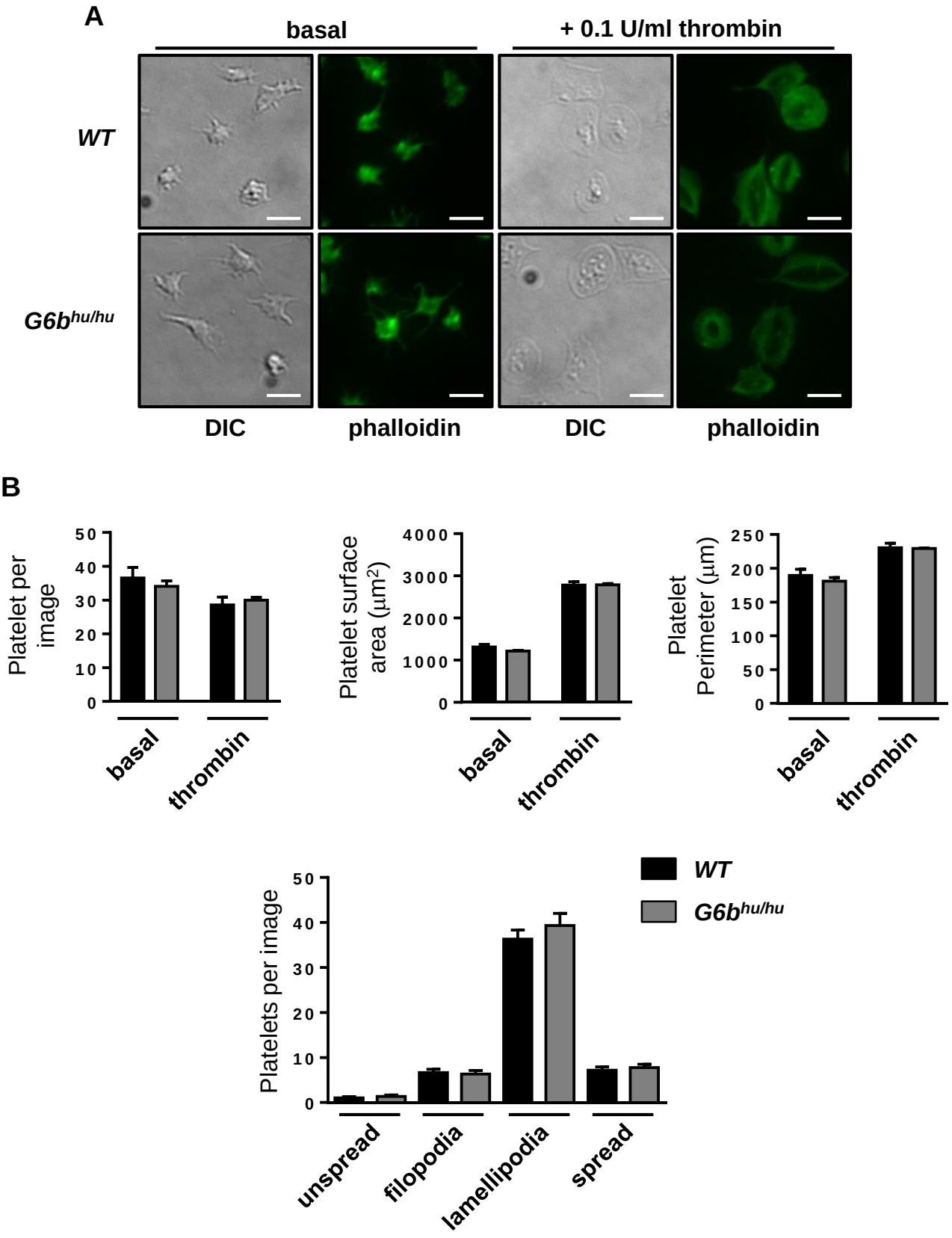

Figure S8. (A) Representative differential interference contrast (DIC) and Alexa-488-conjugated phalloidin stained images of fibrinogen spread washed platelets (2×10^7/mL) under both resting and 0.1 U/ml thrombin pre-activated conditions. (B) Quantification of DIC images in indicated genotypes. Mean ± SEM, n=3.

Figure S9

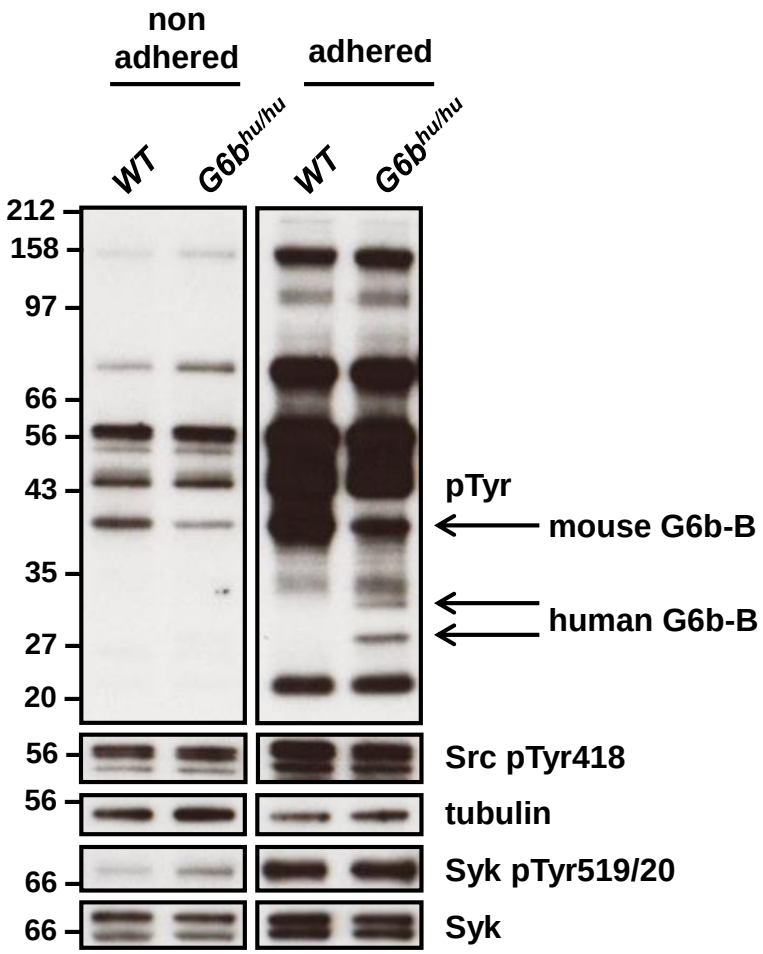

Figure S9. Normal signalling in fibrinogen adhered *G6b*$^{hu/hu}$ washed platelets (4 × 10^8/mL).

Figure S10

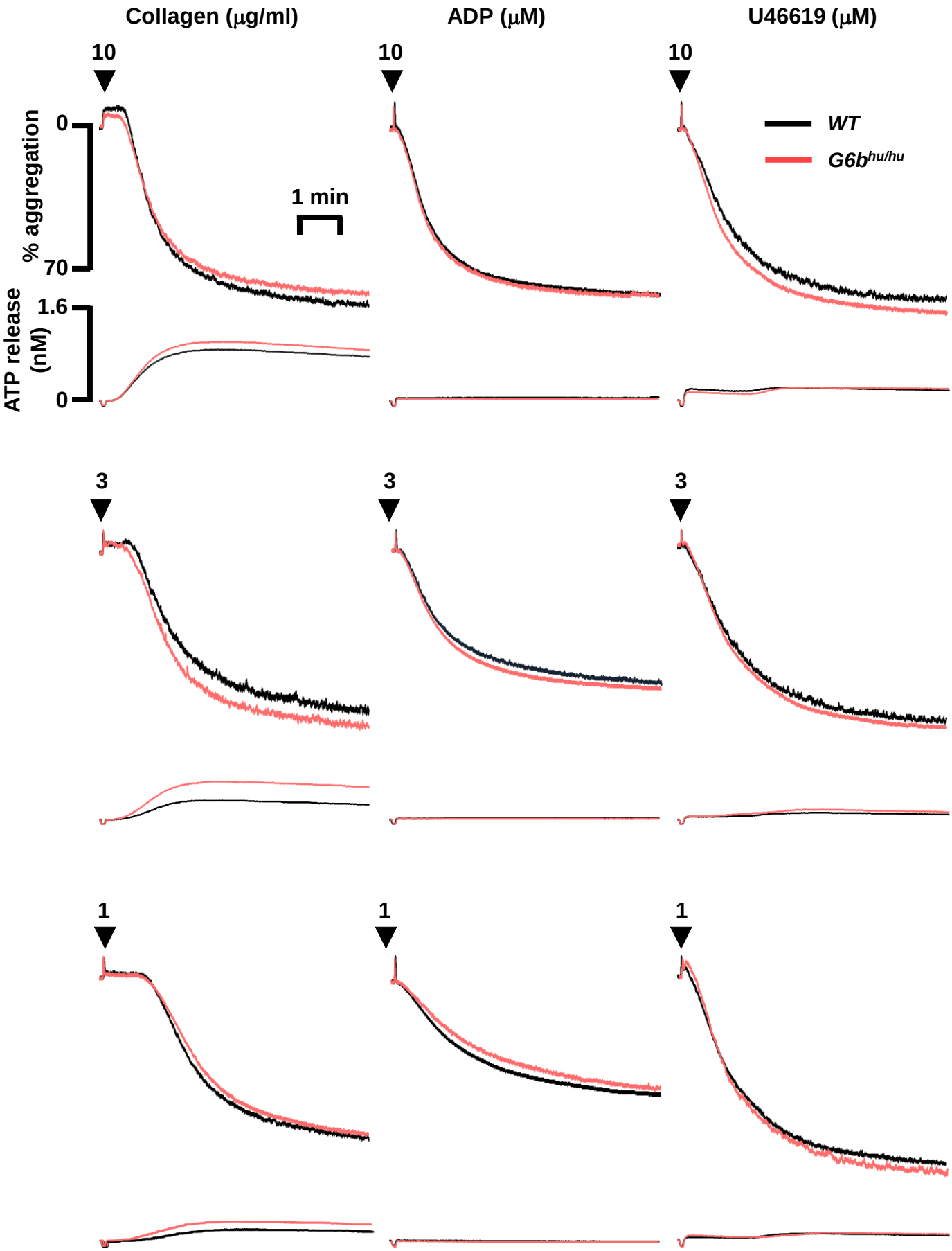
Collagen (μg/ml)
ADP (μM)
U46619 (μM)
10
3
1
% aggregation
0
70
ATP release (nM)
1.6
0
1 min
WT
G6b^hu/hu

Figure S10

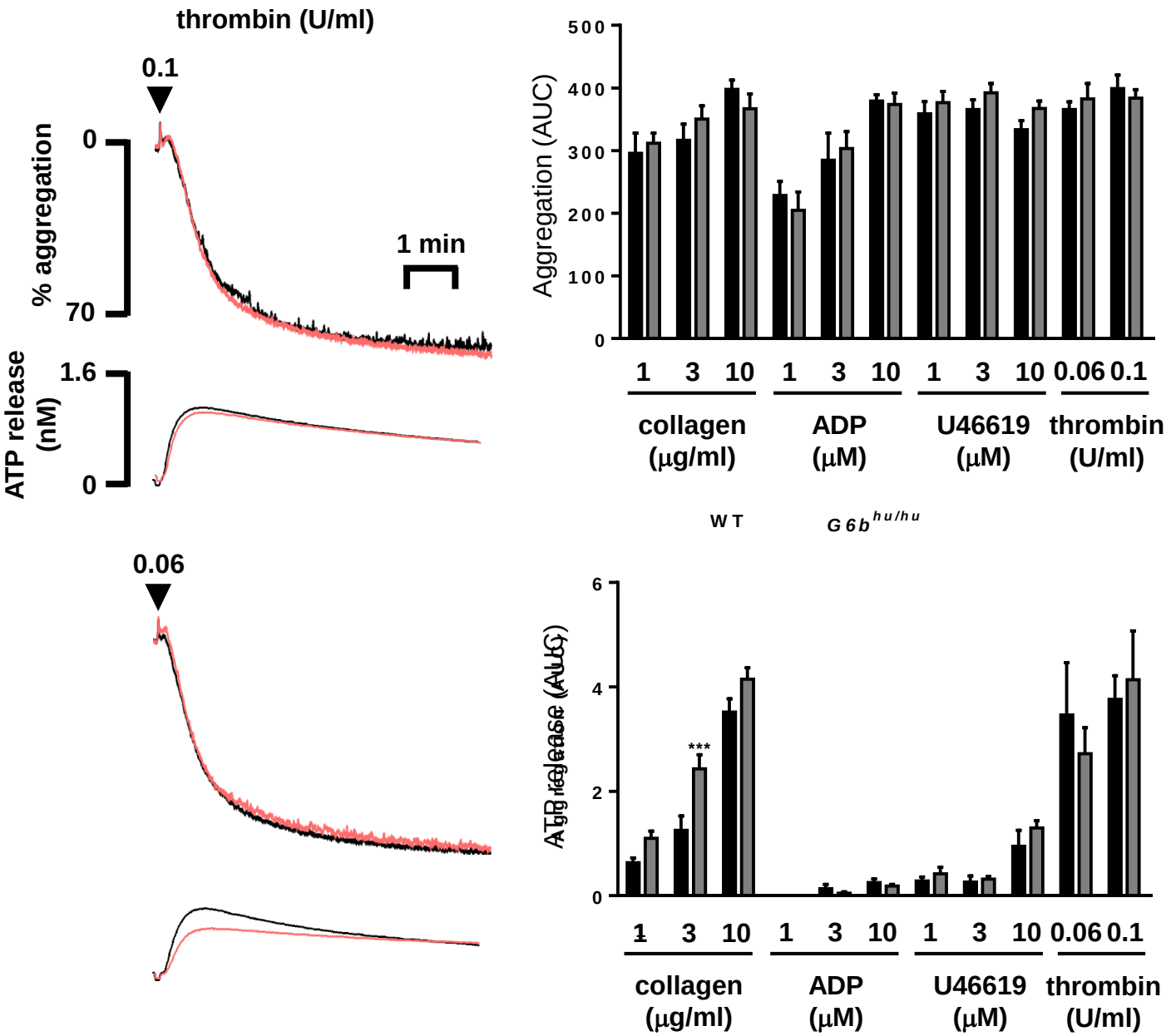

Figure S10. Mean aggregation and ATP release traces for *WT* and *G6b*$^{hu/hu}$ washed platelets (2×10^8/mL) activated with indicated agonists. Area under the curve (AUC) was compared for each of the traces (n=4-6, mean ± SEM, *** P<0.001).

Figure S11

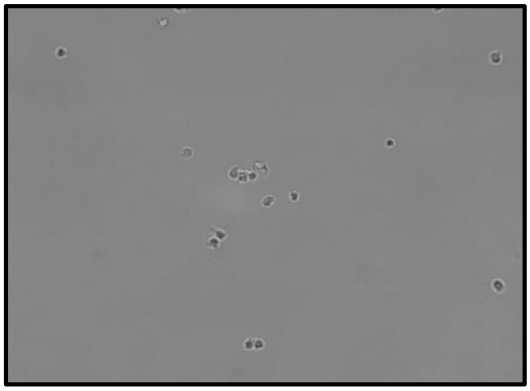

Morphological score – 0
Contraction score – 0
Multilayer score – 0

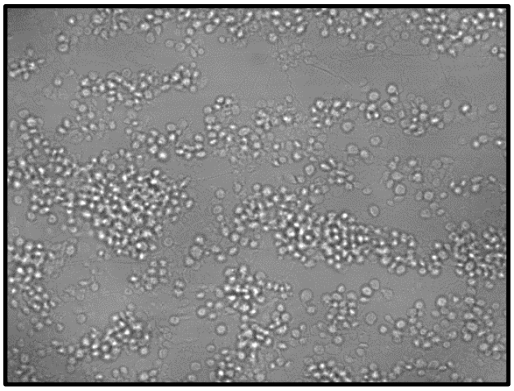

Morphological score – 3
Contraction score – 1
Multilayer score – 1

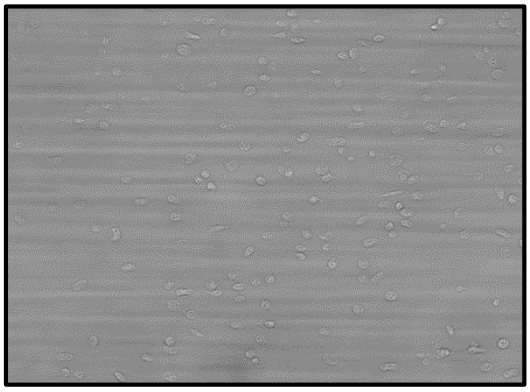

Morphological score – 1
Contraction score – 0
Multilayer score – 0

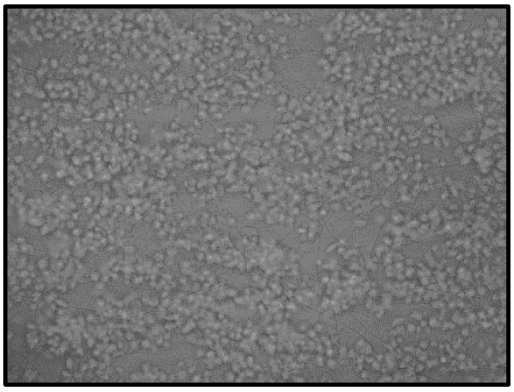

Morphological score – 4
Contraction score – 2
Multilayer score – 2

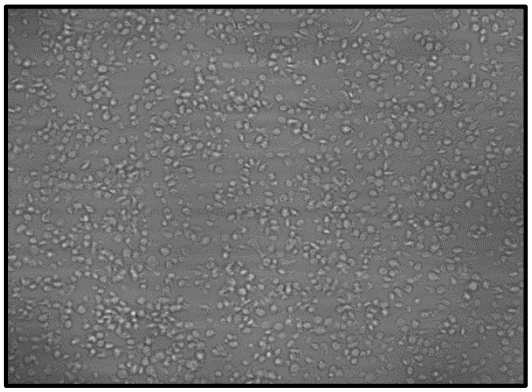

Morphological score – 2
Contraction score – 0
Multilayer score – 0

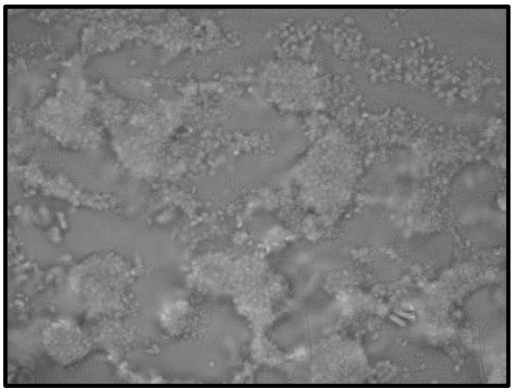

Morphological score – 5
Contraction score – 3
Multilayer score – 3

Figure S11. Platelet flow adhesion morphological scoring representative images

Figure S12

A

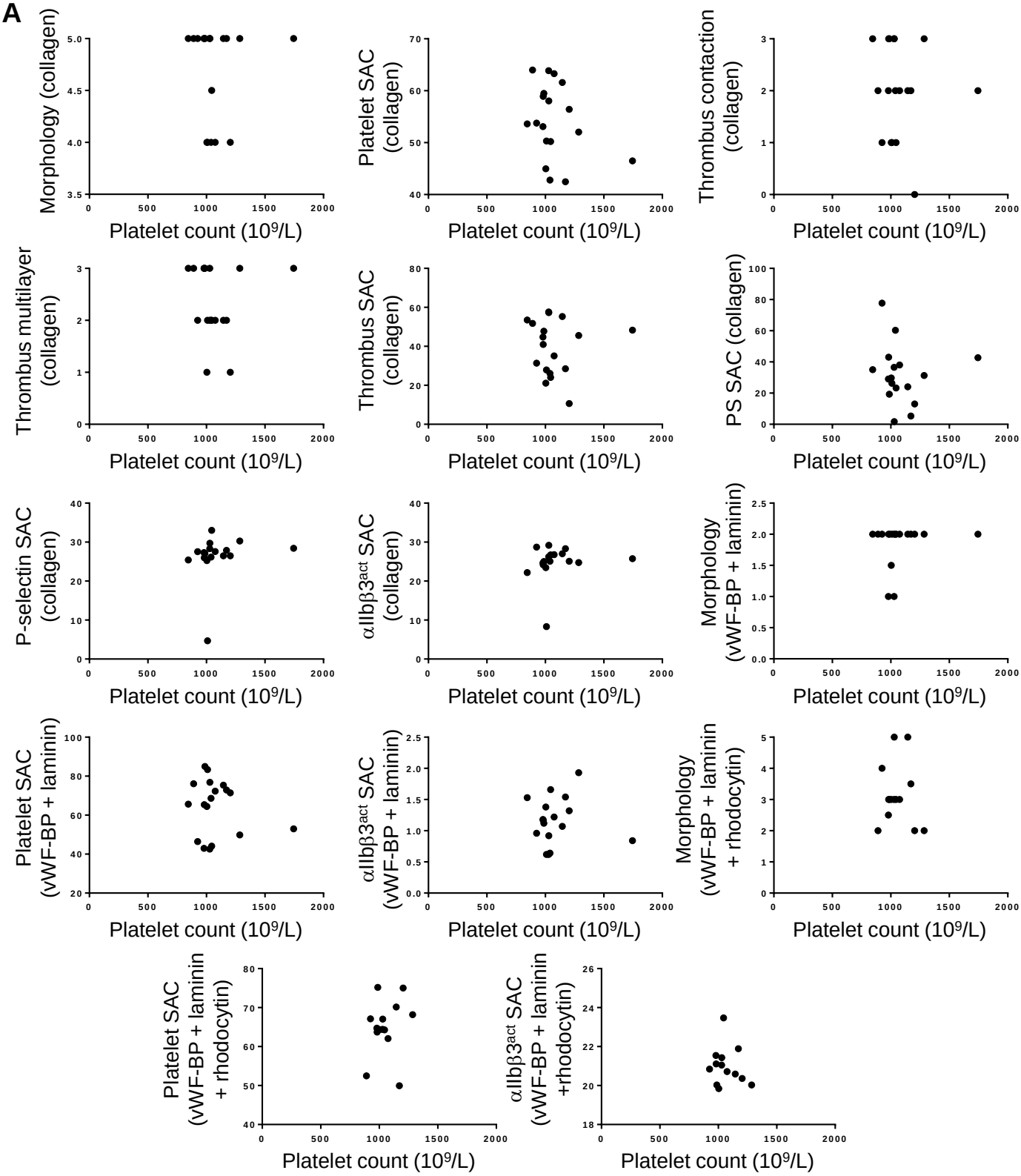

B

	Morphology	Platelet SAC	Thrombus contraction	Thrombus multilayer	Thrombus SAC	PS SAC	P-selectin SAC	αIIbβ3act SAC	Morphology	Platelet SAC	αIIbβ3act SAC	Morphology	Platelet SAC	αIIbβ3act SAC
R^2	0.002	0.1	0.006	9×10^{-4}	3×10^{-4}	0.006	0.032	0.02	0.026	0.029	1×10^{-5}	0.007	0.042	0.026
P value	0.858	0.202	0.763	0.905	0.947	0.763	0.492	0.591	0.52	0.5	0.989	0.778	0.482	0.601
	Collagen								vWF-BP + Laminin			vWF-BP + Laminin + Rhodocytin		

Figure S12. (A) Scatter plots of measured parameters of platelet adhesion and activation against platelet count in a cohort of *WT* mice with platelet counts ranging between 845-1745 × 10^9/L (n=14-18). (B) R^2 and P-values of linear regression models, demonstrating platelet count is not a good predictor of any of the parameters measured.

Figure S13

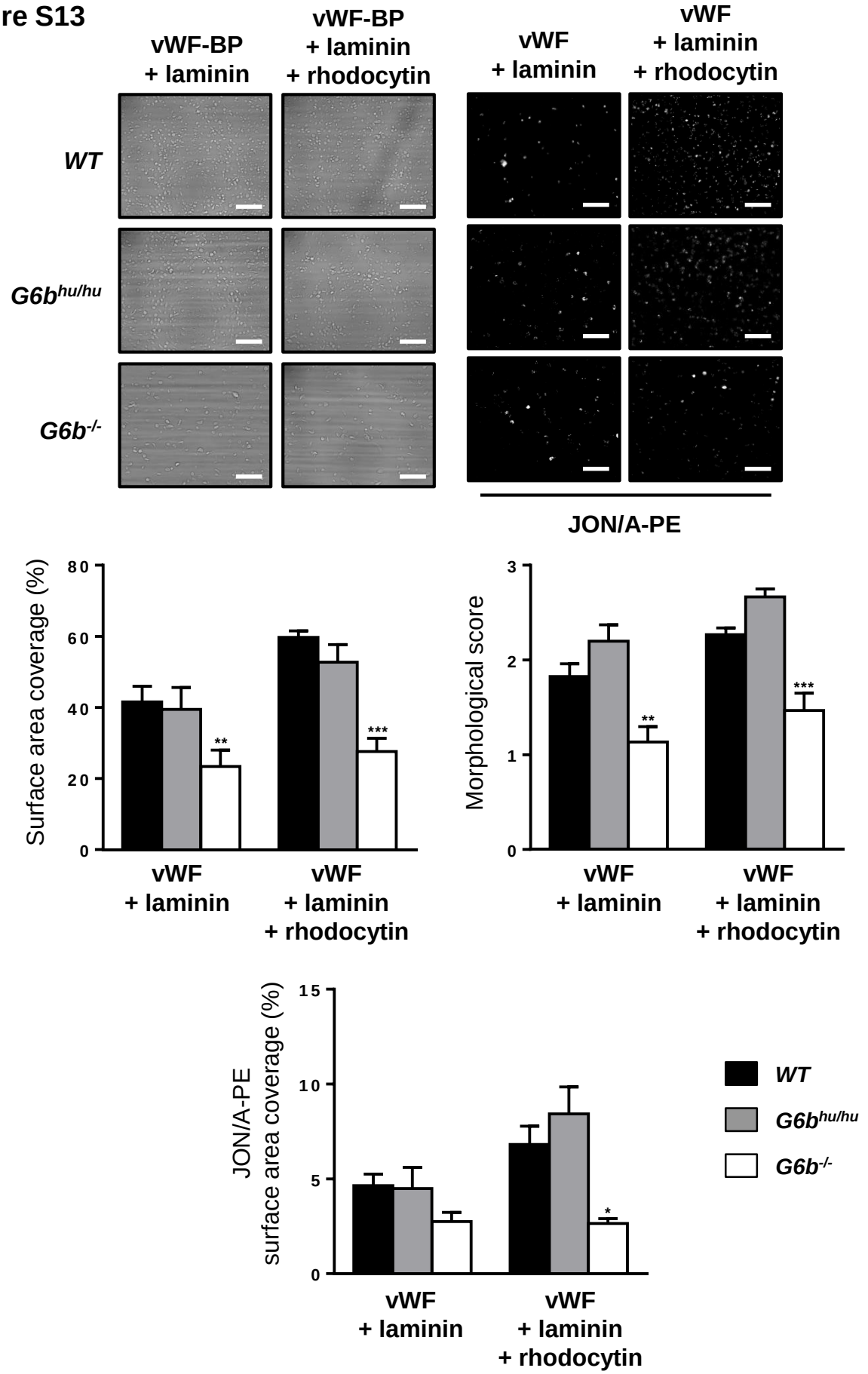

Figure S13. Representative images and quantification of total platelet surface area coverage, morphological score and JON/A-PE surface area coverage of heparin-PPACK-fragmin anticoagulated whole blood flowed over collagen coated coverslips. n=5-6, mean ± SEM, * P<0.05, ** P<0.01, *** P<0.001.

Figure S14

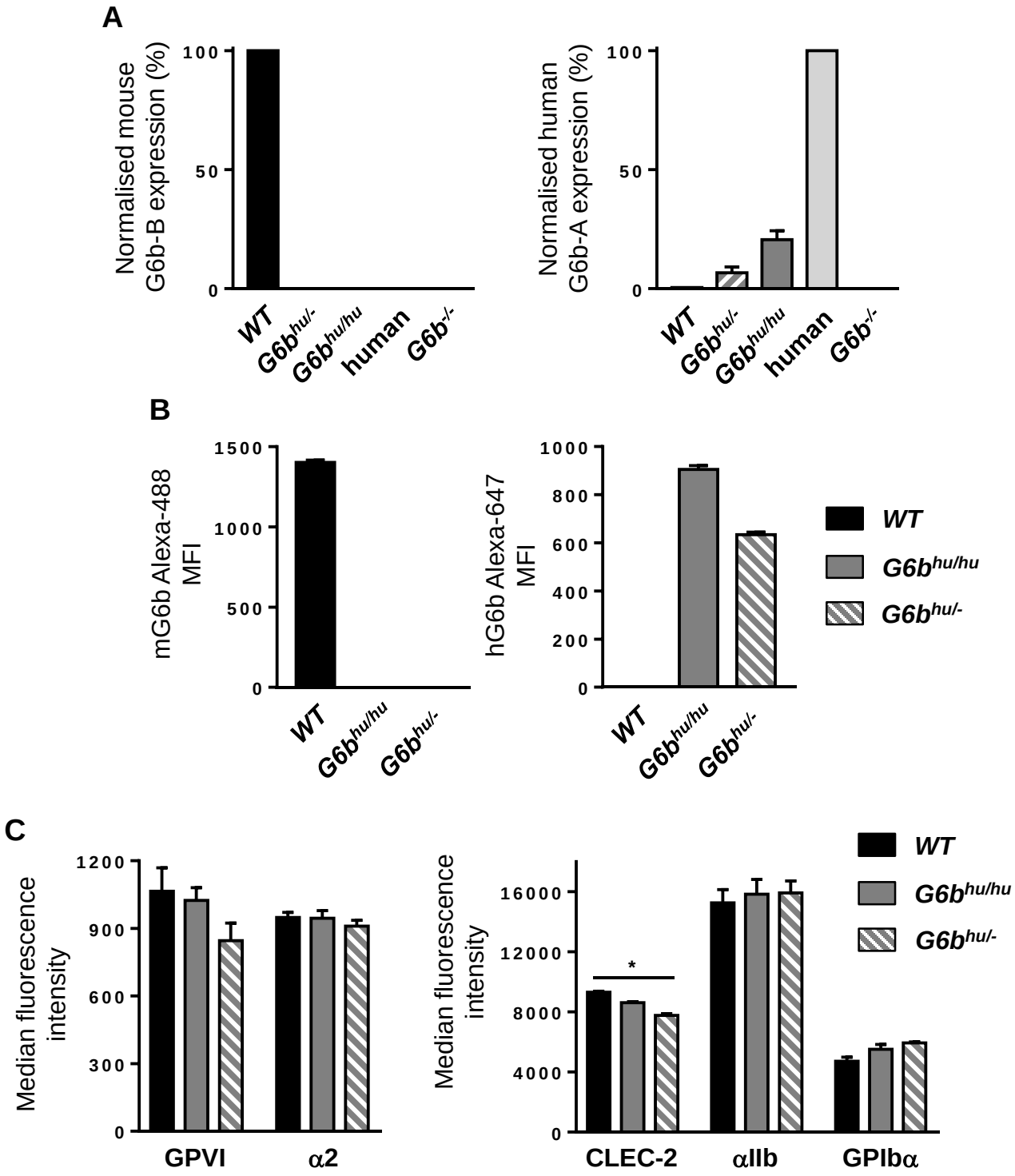

Figure S14. (A) Quantification of mouse and human G6b-A total protein levels in lysates prepared from washed platelets (4×10^8/mL). (B) Surface expression levels of mouse and human G6b. (C) Surface expression levels of major platelet receptors.

Figure S15

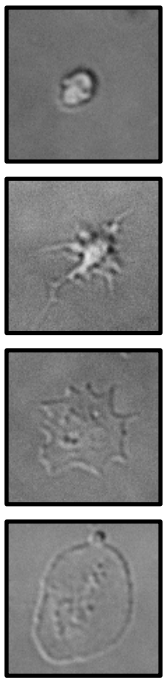

Figure S15. Washed platelet spreading on fibrinogen scoring categories

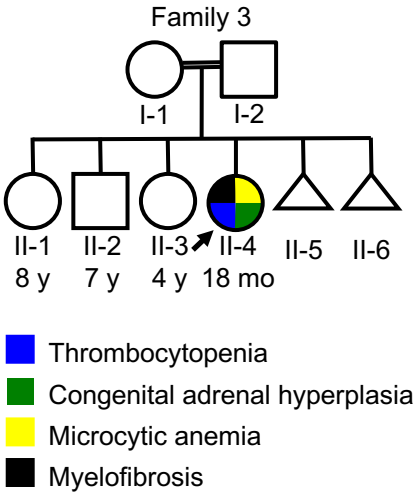
Family 3
I-1
I-2
II-1
8 y
II-2
7 y
II-3
4 y
II-4
18 mo
II-5
II-6
Thrombocytopenia
Congenital adrenal hyperplasia
Microcytic anemia
Myelofibrosis

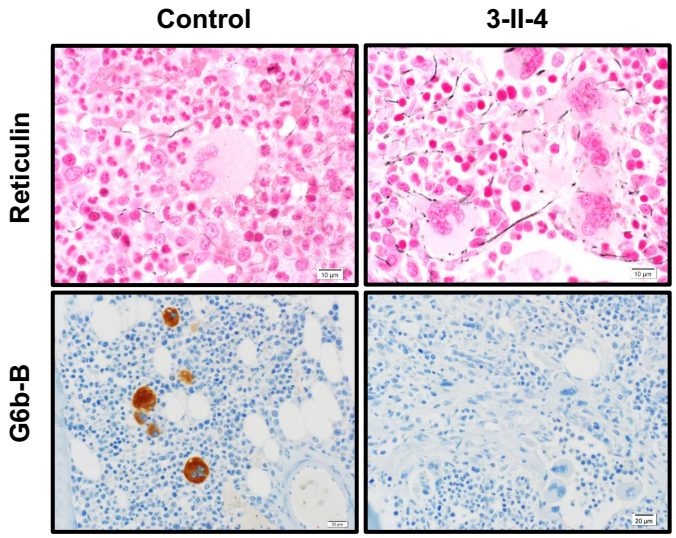
Control
3-II-4
Reticulin
G6b-B

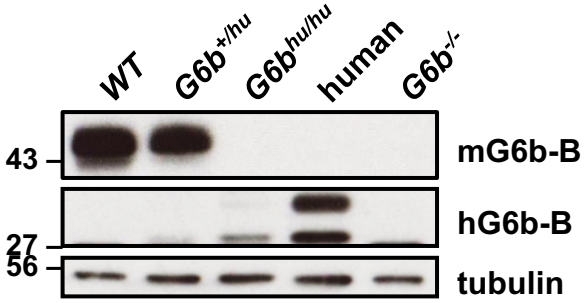
WT
G6b+/hu
G6bhu/hu
human
G6b-/-
43
27
56
mG6b-B
hG6b-B
tubulin

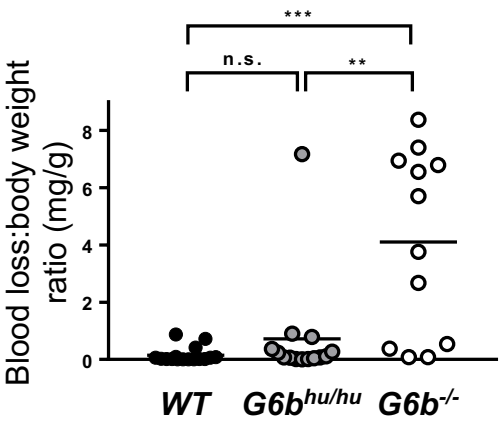
***
n.s.
**
Blood loss:body weight ratio (mg/g)
0
2
4
6
8
WT
G6bhu/hu
G6b-/-